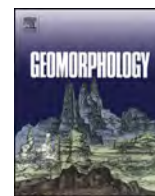




Contents lists available at ScienceDirect

Geomorphology

journal homepage: www.elsevier.com/locate/geomorph

The strong competition between growth and erosive processes on the Juan Fernández Archipelago (SE Pacific, Chile)

Laura Becerril ^{a,*}, Luis E. Lara ^{a,b}, Valentina I. Astudillo ^c

^a Servicio Nacional de Geología y Minería, Avd. Santa María 0104, Santiago, Chile

^b CIGIDEN, Research Center for Integrated Risk Management, Chile

^c Primer Tribunal Ambiental, Avd. José Miguel Carrera 1579, Antofagasta, Chile

ARTICLE INFO

Article history:

Received 6 May 2020

Received in revised form 5 November 2020

Accepted 11 November 2020

Available online xxxx

Keywords:

Robinson Crusoe

Alejandro Selkirk

Growth rates

Erosion rates

Paleo-reconstruction

Submarine geomorphology

ABSTRACT

Ocean Island Volcanoes experience growth and dismantling throughout their entire geological history. When these volcanoes are in their post-shield or post-rejuvenated stage, erosion and subsidence dominate leading them towards a dramatic end, with their extinction as subaerial and transition to the guyot or razed island stage. To quantify the long-term growth and erosion rates affecting these volcanoes is complex but essential to understand the interplay between competing processes, some of them coeval. The emerged parts of the Juan Fernández Ridge (Robinson Crusoe (RC) and Alejandro Selkirk (AS) Islands) in the Pacific south east (Chile), separated ca. 200 km and different in age (ca. 4 and 1 Ma, respectively), are nowadays experiencing a staunch decay. Here we present new data related to the construction and erosion rates experienced by these major islands, whose emerged parts represent a small fraction of their entire volcano edifices.

Based on geomorphological analyses of combined topographical and bathymetrical maps, and the reconstruction of the paleo-topography, we obtained total average long-term growth rates (emerged and submarine sections) that are very similar for the two edifices, between ~1100 and 1500 km³/My, despite their different age and evolutionary stage. Considering only the emerged section of the paleo edifices, or the present island volumes, result in lower growth rates (45–30 km³/My for RC and AS respectively), which are in the same order of magnitude than other oceanic islands worldwide.

Long-term average-basin erosion rates are rather different. RC basins present lower erosion rates (116.77 t/km²yr) than AS (465.75 t/km²yr), which suggest a time-dependent process with RC being closer to the equilibrium profile. These values are in the same order of magnitude than those from other ocean settings with higher rainfall regimes, which would even imply higher erosion rates in Juan Fernández archipelago and a possible role for solid Earth processes that control vertical movements, mass wasting and hence long-term bulk erosion.

These results reveal the need to attempt a fully reconstruction of paleo-edifices, considering also the submerged sections, when emerged parts are intensely eroded, thus aiming for more representative growth and erosion rates estimations as a first step towards understanding processes controlling morphological evolution of oceanic islands.

© 2020 Elsevier B.V. All rights reserved.

1. Introduction

Volcanic islands and seamounts related to hotspots (e.g., Courtillot et al., 2003; Pimentel et al., 2020) are common ocean features where geological processes are highly active and seem to evolve in a more rapid way than their continental counterparts (Ramalho et al., 2013). Their evolution is then a constant competition between magmatism, tectonics and erosion that model their landscapes during their entire geological history (Thouret, 1999; Ramalho, 2011). Specifically, they mainly grow and decay as result of a delicate balance among extrusion and intrusion rates, tectonics associated to subsidence/uplift processes and subaerial and marine erosion and/or mass wasting (Ramalho, 2011).

When magmatism stops, long-term erosion becomes the dominant factor that dismantles these ocean volcanoes, being a process still poorly documented with a few well-known case-studies (Ricci et al., 2015). Many ocean island volcanoes and other volcanic islands related to different tectonic settings elsewhere (i.e. those not purely related to intraplate volcanism), have been studied from a geological/geomorphological point of view, and particularly considering their growth rates. Archetypical example is Hawaii (e.g. Decker, 1987) being a reference for the rest of ocean island volcanoes and seamounts. Previous studies also include: Canary Islands (e.g. Schmincke, 1982; Carracedo, 1999); Galapagos (e.g. Chadwick and Howard, 1991); Reunion (e.g. Carter et al., 2007 and references therein) and Cape Verde (Ramalho, 2011), among others. Some additional contributions aimed to constrain the mechanical and/or total erosion affecting ocean volcanoes over a long-time scale, for example in the West Indies (Le Friant et al., 2004; Samper et al., 2007; Germa et al.,

* Corresponding author.

E-mail address: laura.becerril@sernageomin.cl (L. Becerril).

2010); French Polynesia (Hildenbrand et al., 2008); and La Reunion (Salvany et al., 2012). Very few studies have combined both the estimation of growth and erosion rates, as done by Ricci et al. (2015) for the Lesser Antilles.

Ocean island volcanoes and seamounts in the Pacific Southeast are represented by a number of volcanic alignments some of them with emerged lands forming isolated archipelagos (e.g., Easter Island and the Easter Seamount Chain, San Félix-San Ambrosio, Juan Fernandez Ridge) or completely submerged (e.g., Iquique Ridge, Copiapó Ridge) (Fig. 2). Despite some few works focused on the magmatic evolution of these volcanic islands and seamounts (e.g., Lara et al., 2018; Reyes et al., 2017, 2019; Truong et al., 2018; Paquet et al., 2019), little is known in detail about their geomorphological evolution and controlling factors such as (1) the long-term rates of growth (due to intrusions and eruptions); (2) the long and short-term erosion rates, both due to surficial and coastal processes; and (3) the history of island emergence and subsidence and the magnitude of the vertical movements involved.

In the present study we have performed analyses of topography and bathymetry of the two emerged volcanoes in the Juan Fernández Ridge: Robinson Crusoe (RC) and Alejandro Selkirk (AS) islands. This study is mainly based on a geomorphological analysis of onshore Digital Elevation Models (DEMs) with different resolutions (10–90 m) and multibeam bathymetry (10–900 m resolution) from both satellite altimetry and multibeam surveys. We have reconstructed the paleo-islands (Fig. 1) with the aim to better constrain the constructed and dismantled volumes and their associated My-scale growth and erosion rates. We have also used the existing geochronological catalogue plus the inferred ages of the insular shelves (Fig. 1) and the bottom of volcano edifices (Fig. 1) to calculate time-averaged growth rates. For the long-term erosion rates, we have analysed 29 basins (12 in RC and 17 in AS), to obtain their main basin's morphological parameters and the erosion rates they have experienced during their subaerial geological evolution.

The shield stage at RC Island has been dated at ca. 4 Ma whereas AS is younger and dated at 1 Ma (Reyes et al., 2017; Lara et al., 2018). They define therefore a suitable scenario for a comparative study of growth and erosion rates giving valuable information about their landscape dynamics.

Our aim in this article is three-fold: (1) to show the relevance of attempting paleo-reconstruction of both emerged and submarine portions of ocean volcanoes for first-order estimations of growth and erosion rates; (2) to compare growth and erosion rates in volcanoes with different age and thus contribute to the notion of evolving landscapes and geomorphological equilibrium; and (3) to provide first-order estimations of growth and erosion rates for subsequent more detailed studies of vertical movements and their geological constrains.

Understanding growth and erosion dynamics are of paramount relevance to infer mantle processes and lithosphere response to deformation during hotspot volcanism and could also shed light into surface processes that control the stability of the singular ecosystems and the human habitability in these isolated places.

2. Geographical, geological and geomorphological setting

The Juan Fernández Ridge (JFR) is a ~800-km-long (Fig. 2A), east-west trending (N80°E) volcanic chain of mostly submarine volcanoes (Lara et al., 2018), where RC, SC and AS Islands are the subaerial parts of large shield volcanoes (Fig. 2B). The JFR is related to a hotspot (Farley et al., 1993; Reyes et al., 2017) and is mostly built on top of a ca. 22–37 Ma old Nazca Plate (Rodrigo and Lara, 2014; Lara et al., 2018).

RC Island (formerly Más a Tierra; 33°39'S/78°50'W) and SC islet are part of the same volcanic edifice (area of 49.51 km²) situated ~670 km off the South America's mainland (Fig. 2B, C). This is the most voluminous volcanic edifice of the ridge, although with a modest emerged volume of 12.93 km³ (RC: 12.35 km³ and SC: 0.58 km³). AS Island (formerly Más Afuera; 33°45'S/80°47'W) is larger in surface with a total area of 53.58 km² and a total emerged volume of 28.27 km³ (Fig. 2B, D). AS is located ~180 km west of RC and the age of the emerged shield is consistent with the age progression that result of Nazca Plate eastward displacement at ca. 8 cm/yr (Lara et al., 2018 and references therein). Maximum elevation reaches 916 m (Cerro del Yunque) at RC and 1372 m (Cerro de los Inocentes) at AS (Fig. 2C, D).

The Juan Fernández archipelago has a subtropical Mediterranean climate (Luebert and Plissock, 2012). Mean annual precipitation, considering a period from 1931 to 2017, reaches 973.02 mm (data from www.ine.cl for RC). Rainfall is higher during the winter and varies with elevation and exposure. Elevations above 500 m experience almost daily rainfall, while the western part of RC and SC are quite dry. Mean annual temperature is about 15 °C; prevailing winds are southerly.

Juan Fernández archipelago is still poorly known from a geological point of view, despite the significant knowledge about their endemic biota (Gil, 2003). The first geological outlines for RC and AS were produced by Quensel (1952) and Baker (1967). Subsequent more detailed petrological and geochemical studies of RC were published by Hedge (1978), Baker et al. (1987), Gerlach et al. (1986) and Farley et al. (1993). The first geochronological data for RC was presented by Booker et al. (1967) and Stuessy et al. (1984). Morales (1987) and more recently Astudillo (2014) studied in a more comprehensive way the geology and geomorphology of RC Island. More recent works established a firm geochronology with RC being the oldest island (ca. 4 Ma) and AS (ca. 1 Ma) the youngest one (Fig. 2) (Reyes et al., 2017; Lara et al., 2018), although geological 1:50,000 scale mapping is still in progress. Both islands are mostly formed by sequences that represent their shield stage (Fig. 2C, D). These sequences are composed by basaltic, microbasaltic and picritic lavas with breccia layers and a few interbedded tephra horizons (Reyes et al., 2017). Feeder dykes for the shield stage are clustered in RC with expression as ridges below sea level (Orozco, 2016). Recent studies unravelled the occurrence of rejuvenated volcanism in RC, dated at ca. 800 ka (Lara et al., 2013, 2018; Reyes et al., 2017). Volcanic products of the rejuvenated volcanism are volumetrically low and crop out as vent facies and gently dipping successions of lavas and pyroclastic deposits (Fig. 2C).

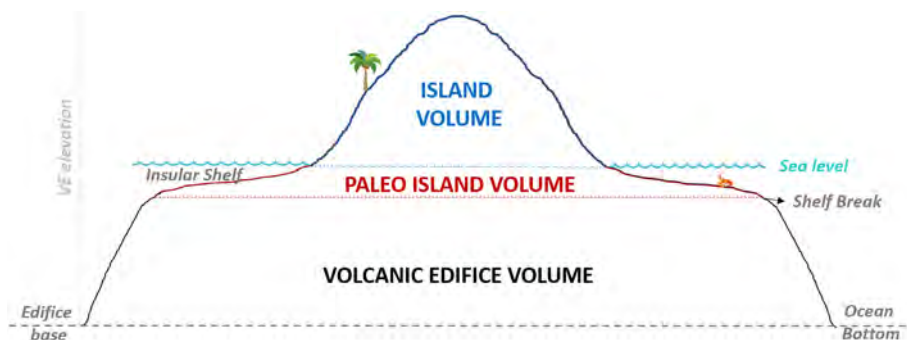


Fig. 1. 3D scheme where concepts used throughout the manuscript such as islands, paleo-islands, volcano edifices shelf breaks, insular shelves, are shown. Note that insular shelves are the base of the paleo-islands.

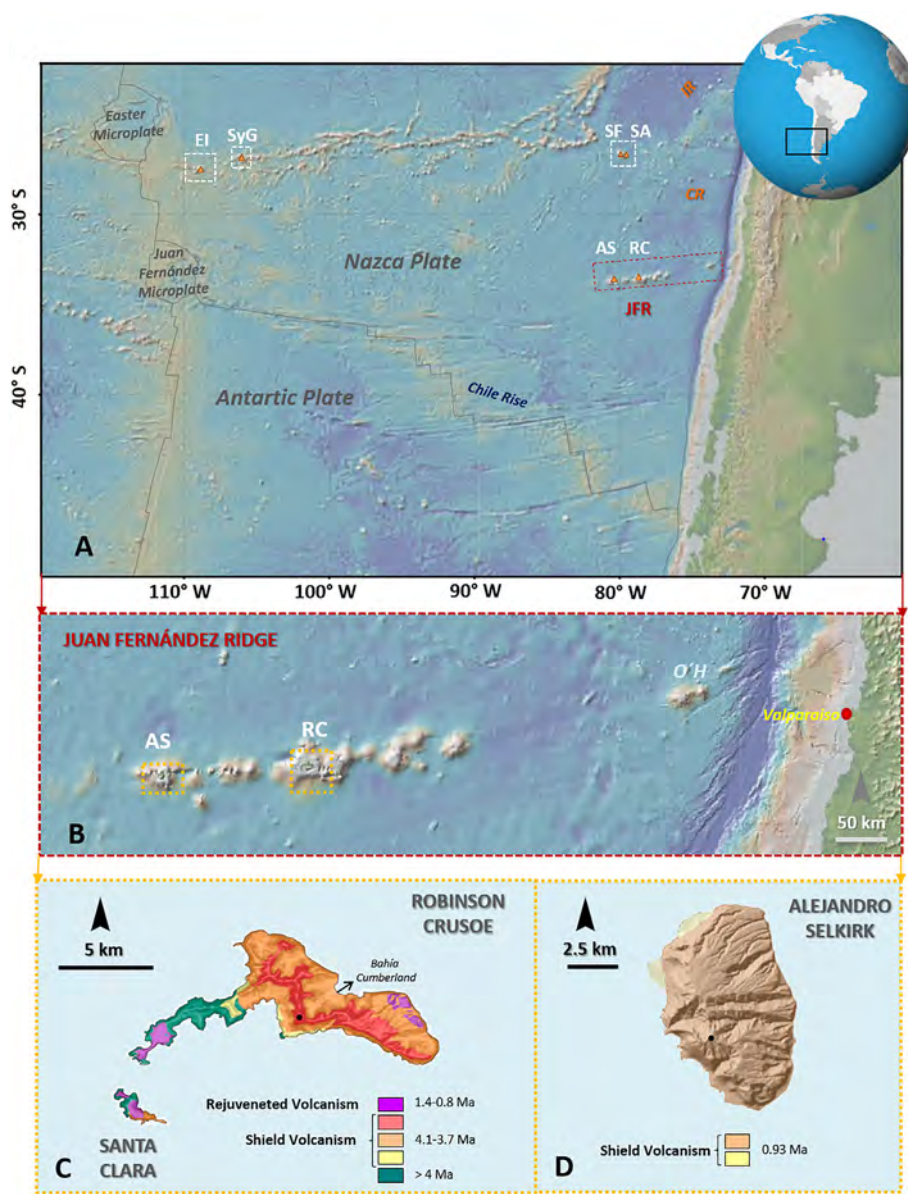


Fig. 2. A) Chilean ocean volcanoes represented by Easter (EI), Salas and Gómez (SyG), San Félix-San Ambrosio (SF-SA) islands, together with the Juan Fernández Archipelago, which is part of the Juan Fernández Ridge (JFR) and is integrated by Robinson Crusoe (RC), Alejandro Selkirk (AS), and Santa Clara (SC) islands. Completely submerged chains are Iquique Ridge (IR) and Copiapó Ridge (CR); B) JFR with AS and RC islands delineated with yellow dashed boxes. O'Higgins guyot is also pointed (O'H); Figures made with GeoMapApp (www.geomapp.org) CC BY (Ryan et al., 2009); C, D) Geological sketch of RC (modified from Orozco, 2016) and AS. Black dots indicate the highest point of each island: Cerro el Yunque (916 m) at RC and Cerro de los Inocentes (1372 m) at AS.

An overview of the JFR geomorphology (Appendix A) reveals that the entire ridge presents advanced erosion with no recent eruptive activity in the emerged components. Despite the occurrence of the rejuvenated stage of volcanism in RC, this island would be in its final erosional stage (*sensu* Schmincke, 2004; Clague and Dixon, 2000 and references therein). Moreover, an historical eruptive event was recently discredited (Lara et al., 2020). On the contrary, AS Island is less eroded but highly incised being in the first erosive stage. These facts make both islands especially suitable places to quantify and compare long-term growth and erosive processes along the same volcano chain.

3. Methodology

We have quantitatively analysed the volcano geomorphology of both RC and AS edifices. Quantitative bathymetric and topographical analyses have been performed for the whole volcano edifices complemented with field investigations consisting of field observations and mapping.

For the analysis, both RC and SC islands have been considered as one since they belong to the same volcanic edifice. AS has been analysed separately.

3.1. Offshore study

3.1.1. Bathymetrical and derived analysis

We compiled bathymetrical data from different sources with diverse resolutions (from ~900 m to 10 m; see Appendix B for more details). Table B.1 shows the different sources for bathymetric products used in this study. To create an integrated 50 m resolution DEM we merged all the available datasets using different interpolation methods with ArcGIS® 10 by Esri, up to getting the best DEM through natural neighbour interpolation method (Fig. 3C, D). We have based the further analysis of this study on these models despite them being incomplete, mainly lacking those proximal areas around the islands. Nevertheless, we have been able to map the main geomorphological features offshore.

From DEM analyses we inferred the shelf break position for both islands that represents the edge, with sharp increase of slope, between the insular shelf and the submarine flanks of the volcanic edifice, and the base of each edifice. We calculated the area and width of the insular shelf, which represent the original pre-erosive islands surface (Quartau et al., 2010, 2015), their long-term enlargement or widening rates, and the total areas and volumes of the whole volcanic edifice. This allowed us to reconstruct the paleo-islands through which we quantified long-term growth, and erosion rates also using geochronological data.

Due to the absence of geochronological data for the submerged parts of the volcanic edifices we have inferred the age of both the insular shelf and the base of each volcano from onshore ^{40}Ar - ^{39}Ar geochronological data. The oldest available onshore age for each volcano edifice was considered as the minimum insular shelf age. By linear regression over the available sequentially taken onshore radiometric data we obtained an empirical age-height curve from which we calculated the maximum summit plateau and the age of the volcanic edifice base as follows:

$$\text{For RC } h = -2140.9a + 8777.7 \quad (1)$$

$$\text{For AS } h = -20223a + 18943 \quad (2)$$

where h is the height (m) of the volcano edifice and a the corresponding age of the sample to this height in Ma.

It should be noted that several assumptions were taken for the calculus: a) constant onshore growth rates, which were extrapolated to the submerged section and therefore similar sequence thicknesses between geochronological samples/data; b) no complex tectonic disturbing the volcanic piles; c) insular shelf age or base of the edifice do not vary spatially (see Section 4.1 for more details).

3.2. Onshore study

3.2.1. Field work and mapping

Several fieldwork campaigns were done in order to get information from the geological, stratigraphic and geomorphological units of the islands. We visited their main drainage basins in order to characterise them and to identify erosive deposits. We also circumnavigated the coast of RC and AS by boat to get a complete picture of the basins and coastal erosion. Topographical maps and aerial photographs provided by SAF (Chilean Aerial Photogrammetric Service; www.saf.cl) and old geomorphological charts and maps (IREN, 1982; Morales, 1987) were used for field mapping and to preliminary delineate the main island's basins.

3.2.2. Digital Elevation Models (DEMs)

Several DEMs from different sources and resolutions were obtained to perform the analyses (from 90 m to 10 m; see Table B.1 in Appendix B for more details). Free DEMs such as ASTER Global Digital Elevation Model V002 (a product of METI and NASA) were downloaded from <https://lpdaac.usgs.gov/products/astgtmv002/>. We first compiled all DEM and then compared them in order to select the most suitable products. Those DEMs with large errors in the vertical component (e.g. CONAF, ASTER, SRTM), with many artefacts (e.g. ASTER GDM or SRTM) or with low resolution were discarded for the further analyses (e.g. AST GTM2; SRTM V2; TANDEM-X) (Table 1; Appendix B).

We finally used the 20 m pixel resolution DEM acquired from SAF products (Table 1, Fig. B.1), created through Finite-Difference interpolation for both islands (Topo to Raster tool in ArcGIS® 10), since it creates a correct hydrological surface (Hutchinson and Gallant, 1999). The 20 m DEM is thus suitable to confidently compare the main morphological

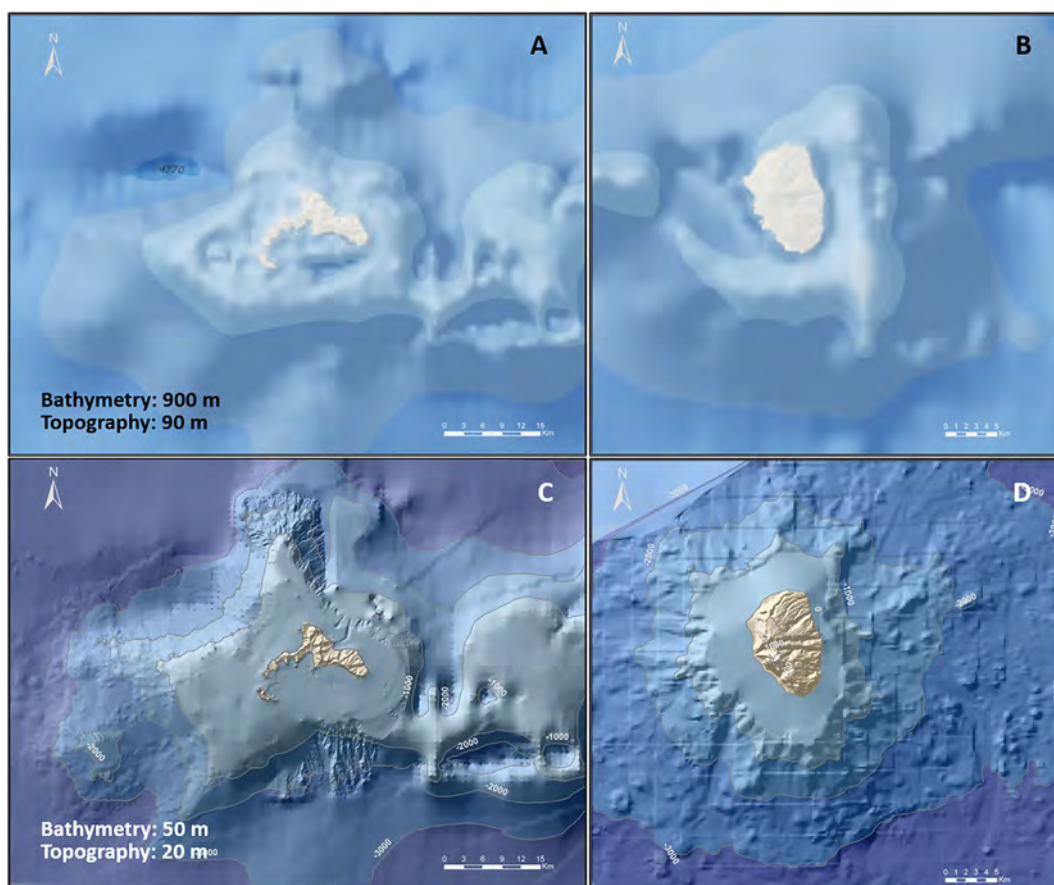


Fig. 3. A, B) Low resolution bathymetrical (GEBCO-900 m resolution) and topographical (ASTER-90 m resolution) maps of AS and RC; C, D) combined medium-high resolution seafloor bathymetry and subaerial topography maps of AS and RC volcano edifices (combined resolutions maps range from 10 m to 50 m).

Table 1

Parameters related to the shelf breaks, insular shelves, islands, paleo-islands and volcano edifices. Estimated values for RC include Santa Clara Island. ⁴⁰Ar/³⁹Ar ages published by Lara et al. (2018). See Fig. 1 for better understanding.

	Age/inferred age (Ma)	Depth (m)	Min/max width (km)	Widening average (km/Ma)	Widening average (km ² /Ma)	Area (km ²)	Volume (km ³)	Elevation (m)
RC								
Shelf break -insular shelf	4.19	−200	2.8/14.5	3.35	140.9	610.11	–	–
	4.33	−510						
Island	4.10 ± 0.09*	–	–	–	–	49.51	12.93	916
Paleo-island	4.33	−510	–	–	–	610.11	472.55	1732
Volcano edifice	5.7	−3400	–	–	–	3390	6392	4316
AS								
Shelf break - insular shelf	0.945	−175	1.2/4.8	5.05	161.1	152.31	–	–
Island	0.93 ± 0.02*	–	–	–	–	53.58	28.27	1372
Paleo-island	0.945	–	–	–	–	152.31	64.95	1400
Volcano edifice	1.08	−2900	–	–	–	1397	1658	4520

characteristics of the two volcanic edifices and provides higher accuracy reducing errors since we are working in small-scale areas (less than 50 km²). DEMs were projected to the WGS84 UTM 17S coordinate system.

3.2.3. Hydrological study

We used hydrology tools from ArcGIS® 10 software to perform hydrological analyses. To define the biggest and more representative watersheds of the islands, those with flow accumulation threshold of 1000 were selected for further parameter analysis. After that we re-delineated and smoothed the basins according to the topographical contours using orthophotographs. Hypsometric curves were obtained to assess and compare the geomorphic development basins state through CalHypso GIS extension for ArcGIS (Pérez-Peña et al., 2009). Concave hypsometric curves characterise basins in old stage; s-shaped curves are related to a maturity stage; and convex hypsometric curves are typical of a youthful stage (Strahler, 1953).

Different coefficients such as the Hypsometric Integral (HI), kurtosis (k), skew (s), density kurtosis (dk) and density skewness (ds) were also analysed since they can be interpreted in terms of erosion, basin slope and to quantify changes in the morphology of drainage basins (Harlin, 1978; Luo, 2000; Pérez-Peña et al., 2009 and references therein). The hypsometric integral (HI) represents the area under the hypsometric curve and is related to the size, shape, and relief of the basin as well to other factors such as dominant erosion processes, lithological resistance and/or tectonic uplift rates (Lifton and Chase, 1992; Hurtrez and Lucazeau, 1999; Chen et al., 2003). Based on the HI, a landscape can be classified in terms of the evolution as youthful (HI > 0.5), mature or in equilibrium (HI = 0.5) or old (HI < 0.5) (Strahler, 1953). The skewness (s) represents the amount of head ward erosion in the upper reach of the basin, while the density skewness (ds) denotes the slope change rate (Harlin, 1978; Luo, 2000; Pérez-Peña et al., 2009). When ds has a positive value it is associated with typical fluvial landform (Luo, 2002) and consequently with more active erosion. On the contrary, negative values are associated with sapping landforms (Luo, 2002), and therefore with less erosion. The kurtosis (k) can be interpreted as the erosion on both upper and lower reaches of a basin, while density kurtosis (dk) illustrates mid-basin slope (Harlin, 1978; Luo, 2000; Pérez-Peña et al., 2009).

3.2.4. Surface analyses - morphological parameters

We used the 20 m resolution DEM as a basis to create several derived products such as slope, hillshade, and flow accumulation maps, from which we extracted the main streams of each basin using ArcGIS® 10 software. With these products we were able to obtain basic data about the physiography of the basins. Morphological parameters obtained were: orientation of the drainage basin; maximum and mean slope (S, °); maximum high (H, m); perimeter (P, km); river maximum length (L, km); area (A, km²); mean width (W, m). We have also calculated other parameters that reflect the basins' evolution in terms of erosion as previous studies did for Tahiti-Nui (e.g. Hildenbrand et al., 2008) and Gran Canaria (Menéndez et al., 2008). Thus, the shape factor Rf

(A/L²) and the Gravelius compactness coefficient Kc (0.28P/A^{1/2}) were calculated. The first represents the relation between the size/area of a basin and the length of the main river/stream and affords an indicator regarding the circular character of the basin; the second expresses the shape discrepancy between a given basin and a circle having the same area. Gravelius coefficient is 1 for an ideally circular watershed and increases with both, basin elongation and irregularity of basin boundaries (Sassolas-Serrayet et al., 2018 and references therein).

Since our island's basins are mostly small and narrow, we also calculated a parameter introduced by Hildenbrand et al. (2008) for this kind of basins called relative width w (W/L). This parameter considers variations in the planar shape of a basin along two main directions and evaluates the contribution of longitudinal stream incision and lateral slope denudation during the formation and the evolution of the basins. We calculated the mean width as the average of 20 basins' width measurements, performed at regularly spaced points and perpendicularly along the main river.

3.2.5. Islands/basins paleo-reconstruction and estimated volumes

With the aim to better constrain the constructed and dismantled volumes and the associated growth and erosion rates, two complementary methods were used to reconstruct the paleo-relief of the islands and their basins. First, we combined DEMs from the submerged and emerged parts to calculate the total edifice volume. For the first paleo-topographic reconstruction method we used maximum basin elevations to construct an artificial reference surface extending contour lines up to closing the basins. Once obtained, we subtracted the paleo-basins that represent the upper reconstructed surfaces from the current basins that are the lower surfaces yielding the total volume removed by erosion with the tool Surface Difference (ArcGIS® 10). In this case we assume minimum paleo-heights and therefore minimum volumes were obtained. In the second reconstruction, we restored the pre-erosion geometry of a hypothetical conical volcanic edifice following the methodology described in Hildenbrand et al. (2008). In our case, we used the shelf break obtained through bathymetrical analysis as the original 0 m level (see bathymetrical analyses and Section 4.1 for more details). We calculated the centroid of this surface and extrapolated mean dips and slopes of the island's sequences up to their interjection. That point, located close to the current centre of each island, was used as a maximum elevation for each paleo-island. To estimate the maximum former island height, we also used the empirical relation provided by Vogt and Smoot (1984) and used by Mitchell (2001) where a logarithmic least square regression is used following the equation:

$$\log h = 2.5 + 0.25 \log A \quad (3)$$

with h the maximum island height and A the guyot area that in our case is given by the area of the insular shelf. In the case of AS, we also used some current heights as input for its paleo reconstruction since the island still preserves some original slope surfaces.

The two methods used provide minimum and maximum volumes giving a range of values from what an implicit nominal uncertainty is derived. Thus the uncertainty of the reconstructed edifices is the standard deviation (σ_v) of these minimum and maximum values.

3.3. Long-term growth and erosion rates

3.3.1. Long-term growth rates

For estimating mean long-term growth rates, i.e., the growth rate during the entire life of the volcano edifice or the paleo-island, we have firstly calculated the (1) total volcano edifice volumes and (2) the volume of each paleo-island with the tool Surface Volume in ArcGIS® 10. This tool calculates the area (A) and volume (V) of the volcano edifice or the paleo-island between a surface (the paleotopography) and a reference plane that in this case is the base of the edifices at the seafloor and the insular shelves position, respectively. Based on a preliminary mapping we have also estimated the volume of the rejuvenated stage for RC and we have subtracted it from the total calculated volume to obtain the volume for the shield stage. Once volumes were obtained, we considered the estimated ages (Δt) of the edifice base for each volcano or the inferred age of the insular shelves (see Eqs. (1) and (2) in Section 3.1). Growth rates were simply obtained applying the equation:

$$GR = V/\Delta t \text{ results given in } (\text{km}^3/\text{My}) \quad (4)$$

3.3.2. Long-term erosion rates

After constructing the initial (paleo-island topography) and having the present topography of both islands, we have calculated total and

by basin long-term erosion rates subtracting both topographies and then considering the removed (calculated) volume V, the 3D area of each basin A_b and the time between the construction of the initial topography and the current one Δt , following the equations:

$$Er = V/\Delta t \text{ results given in } (\text{km}^3/\text{My}) \quad (5)$$

$$Er = (V/A_b)/\Delta t \text{ results given in } (\text{m}/\text{My}) \quad (6)$$

A third way to obtain long-term erosion rates is given by the equation:

$$Ev = \rho_r V/A_b \Delta t \text{ results given in } (\text{t}/\text{km}^2\text{yr}) \text{ (Ferrier et al., 2013)} \quad (7)$$

where the density of the eroded material ρ_r has been considered as 3 g/cm³ for basalts, that are the prevalent materials that form RC and AS. Erosion rates are given in different units to make them afterwards comparable with those calculated in other volcanic islands of the world.

4. Results

4.1. Offshore study - bathymetrical and derived analyses

From the combined bathymetrical maps (50 m resolution final offshore map), we have been able to identify the position of the shelf break on both islands (Fig. 4). The shelf break is locally identified as a notable change of the slope corresponding to the edge between the insular shelf and the submarine flanks of the volcanic edifice. It has commonly an erosive origin, sometimes modified by sedimentary, volcanic and mass wasting processes (Quartau et al., 2010, 2014). In those

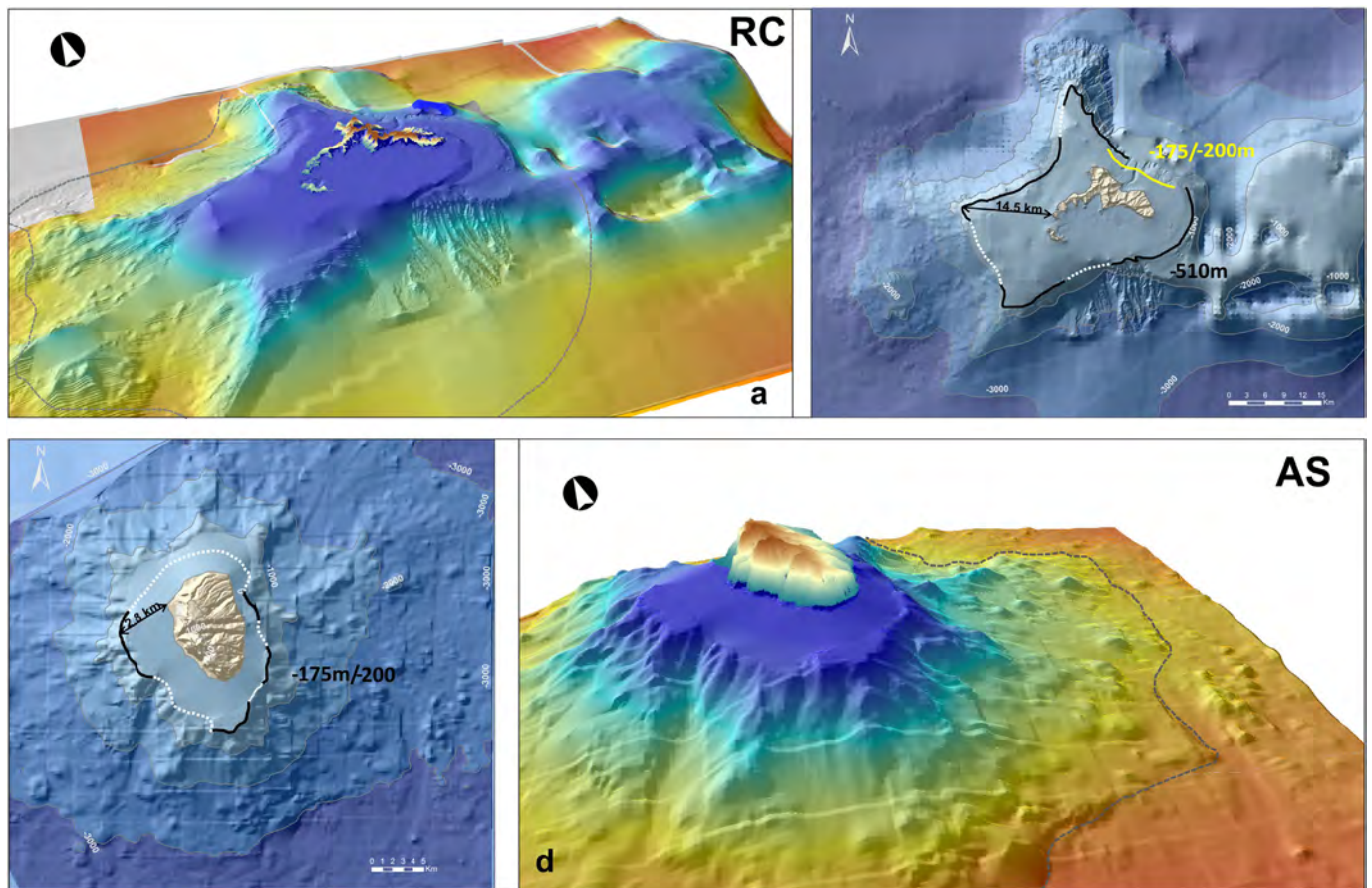


Fig. 4. Shelf break (black and white dashed lines), insular shelves and ocean bottom location (dark grey dashed line) of the volcano edifices of RC (a, b) and AS (c, d). Black arrows with distance in km show the maximum width of the insular shelves in each case.

areas around the islands where bathymetry lacks, we have inferred its position by continuation of the contour between identified points (Fig. 4B, C). For RC two different shelf breaks are distinguished, one at around ~ -510 to 550 m and other, only identified at the northeast of the volcano edifice, between ~ -175 m and -200 m depth (Fig. 4A, B; Table 1). The shelf break in AS is located between ~ -175 m and -200 m depth (Fig. 4C, D). The uppermost insular shelves are significantly below sea-level during the last glacial maxima (~ 130 m), thus implying significant subsidence. Identified sections of shelf breaks on both volcanoes are roughly irregular, sometimes affected by decametre-scale submarine channels/canyons heads (Figs. 4, 5; A.1), and oriented parallel to the present shoreline. The north-western shelf section of RC has a semi-circular concave shape probably related to a submarine mega landslide (Figs. 4, 5; A.1). Insular shelves around both islands have variable widths. The minimum and maximum insular shelves widths are 2.8 km and 14.5 km for RC, and 1.2 km and 4.8 km for AS (Table 1). The

widest shelves are those located at the southwest in both islands (Fig. 4). In terms of total areas RC has an insular shelf of 610.11 km² and AS of 152.31 km² (Table 1). The slope of the insular shelves is mostly less than 5° for both islands. Some profiles have been done in those areas of almost continuous insular shelves (Fig. 5). Fig. 5-Profile A in RC shows a mean slope of 5.38° and a certain roughness close to the end of the platform. Blue line in Fig. 5 shows a step in the profile that corresponds to an error due to an interpolation effect. Profile B is flat and has a mean slope of 2.76° . Profile C in AS shows a gentle mean slope of 4.80° . Profile D represents a parallel section of the insular shelf showing a certain roughness along the profile and a difference of high of only 10 m along 4000 m (Fig. 5).

To accurately use the published ages (Lara et al., 2018) and thus to obtain an age-altitude relation we constructed a schematic section for RC (Fig. 6). We projected the available ages according to the topographic location of the sampling sites. Taking into account the preliminary

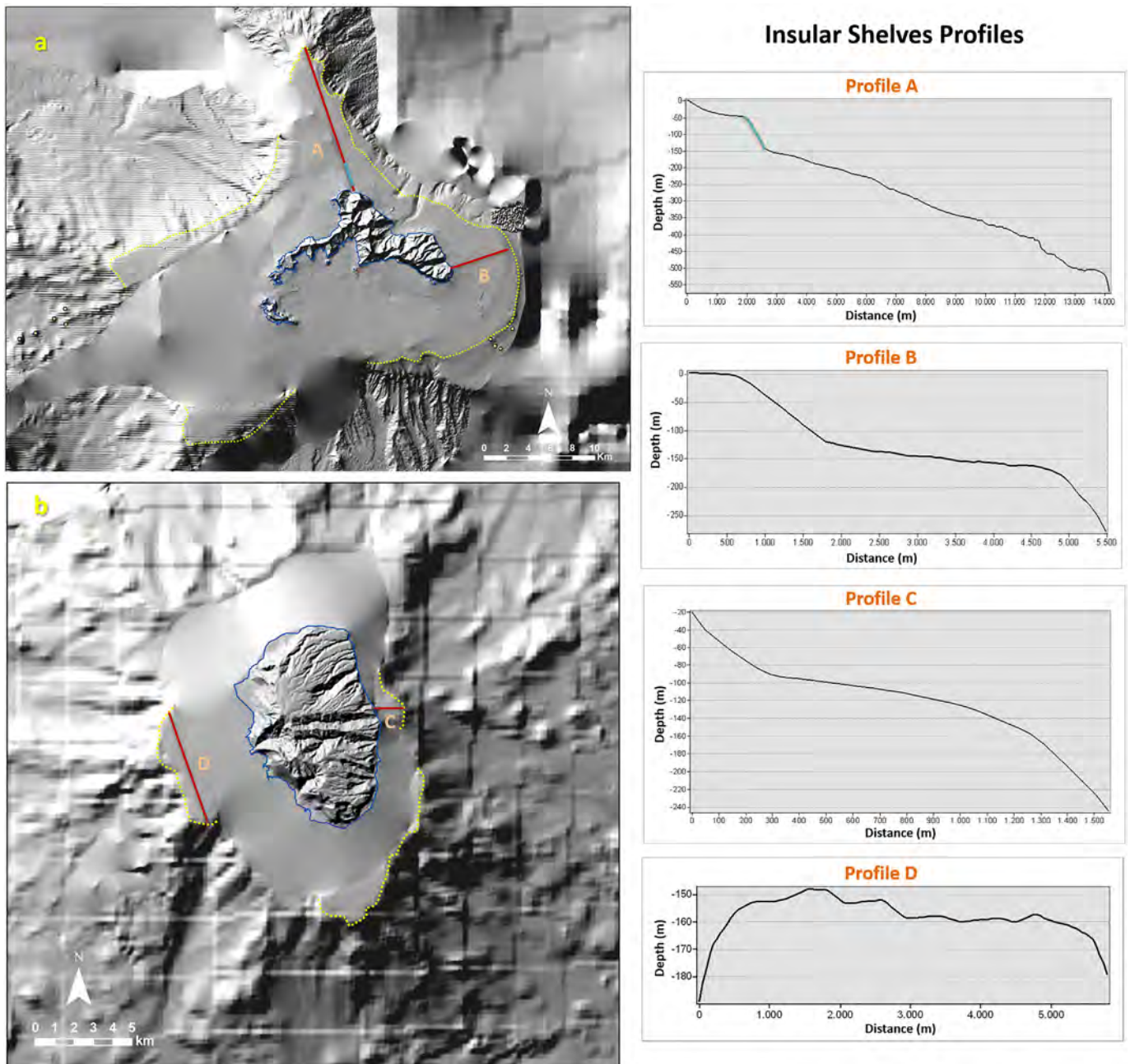


Fig. 5. a, b) Identified shelf breaks and topographical profiles (A–D) of the insular shelves in RC and AS. Yellow dashed lines show the identified shelf break of each island. See text for detailed information.

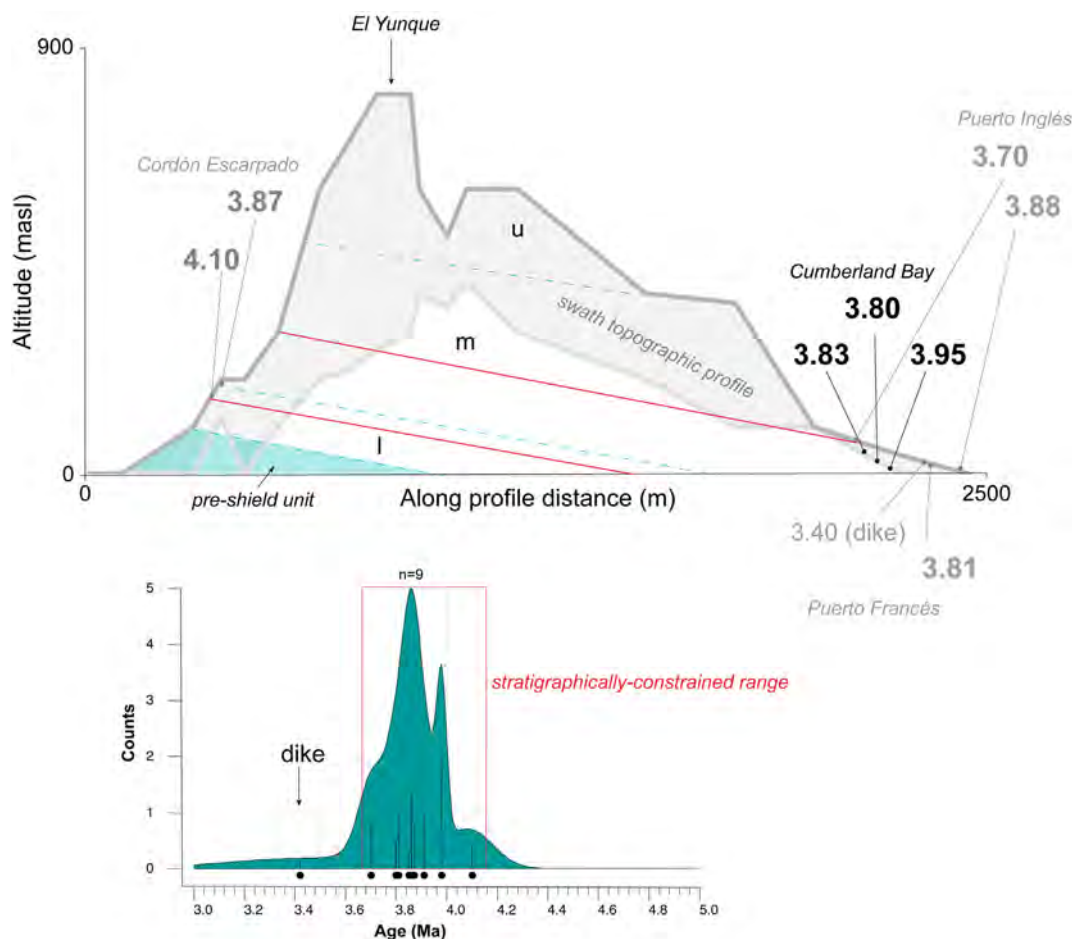


Fig. 6. (a) Schematic 4 km wide swath topographic profile orthogonal to the homocline formed by the stack of lavas forming the shield sequence, near the Cumberland Bay in RC island (see in Fig. 2). Maximum and minimum values are shown for topographic reference. Dips are the true values measured in the field ($\sim 20^\circ$ North). Informal stratigraphic units proposed by Morales (1987) are indicated as l (lower), m (medium) and u (upper) separated by dashed light blue lines. $^{40}\text{Ar}/^{39}\text{Ar}$ ages published by Lara et al. (2018) are projected according to their stratigraphic position. Values in grey for samples collected in valleys nearby, projected onto the profile keeping their topographic and stratigraphic position. Red lines show the stratigraphic range better constrained by the ages. Some minor inconsistencies arise although the difference is within the uncertainty range. (b) Probability density plot with the available ages including a dike dated in ca. 3.4 Ma ($n = 9$) (drawn with DensityPlotter by Vermeesch, 2009). This dyke has a shield stage affinity (Reyes et al., 2017) and could be close to the age of the upper unit (see text for discussion) not already sampled. Red box for the stratigraphically-constrained range shown in the upper panel.

mapping and stratigraphy, samples were located in a stratigraphic context following the dip of the shield sequence ($\sim 20^\circ$ North), which would be composed by three concordant members (Morales, 1987). Maximum and minimum elevations along a swath profile were drawn to better constrain the age range in a topographic context (Fig. 6). We thus obtained that the maximum age of 4.1 Ma is in the lower member and close to the base of the shield unit, which overlies a loosely known and strongly altered pre-shield unit. The minimum age of 3.7 Ma is instead in the middle part of the middle member, about 162 m above the maximum age. This is a feeder dyke of lavas dated in ca. 3.8 Ma. The upper member eluded sampling and hence the age of the sequence is mostly based on the middle member. A dyke dated in 3.4 Ma, with the typical geochemical signature of the shield stage (Reyes et al., 2019) could be interpreted as the age of the upper member and therefore the minimum age of the sequence.

Considering the available onshore ages, we estimated the maximum insular shelf age using Eqs. (1) and (2). Since shelf breaks are located at depths of -200 and -510 m in RC, and -175 m in AS, we obtained the following ages: 4.19 Ma, 4.33 Ma and 0.945 Ma, respectively. These ages allowed us to quantify the maximum enlargement rates of both islands' shelves, i.e., the long-term average rates of shelf widening, that correspond to 3.35 km/My (0.0033 m/yr) in RC, and 5.05 km/My (0.005 m/yr) in AS (Table 1). In terms of area the average widening corresponds to 140.9 km²/Ma in RC and

161.2 km²/Ma in AS (Table 1). We also delimited the base of both volcanic edifices being at -3400 m and -2900 m depth for RC and AS, respectively (Fig. 4A, D; Table 1) and calculated their area (RC: 3390 km²; AS: 1397 km²), and their total present volume (RC: 6392 km³; AS: 1658 km³) (Table 1). Using the Eqs. (1) and (2), we have also calculated the maximum age of the edifice base (at the bottom of the ocean), obtaining an age of 5.68 Ma for RC and 1.08 Ma for AS (Table 1). The total current maximum elevation from the seafloor of the volcano edifices is around 4300 m for both islands (4316 m for RC and 4272 m for AS).

4.2. Onshore study

4.2.1. Hydrological study and morphological parameters

We have identified 12 main drainage basins in RC and 17 in AS (Fig. 7; Table 2). SC islet does not present any basin due to its reduced area. Only those basins greater than 0.5 km² have been considered for the analysis. RC has nine basins more than 1 km², whereas AS has twelve (Table 2). At least ten basins in RC (IDs 1–10 in Tables 3, 4) and five in AS (IDs 1, 4–6, 12 in Tables 3, 4) have sediments that we collected for further analyses. Villagra (ID 1 in Tables 3, 4) and Cumberland (ID 2 in Tables 3, 4) (Fig. 7D, E) basins could have had sub-basins but since all the streams/water lead into the same bay, we have only considered the major ones for the analysis.

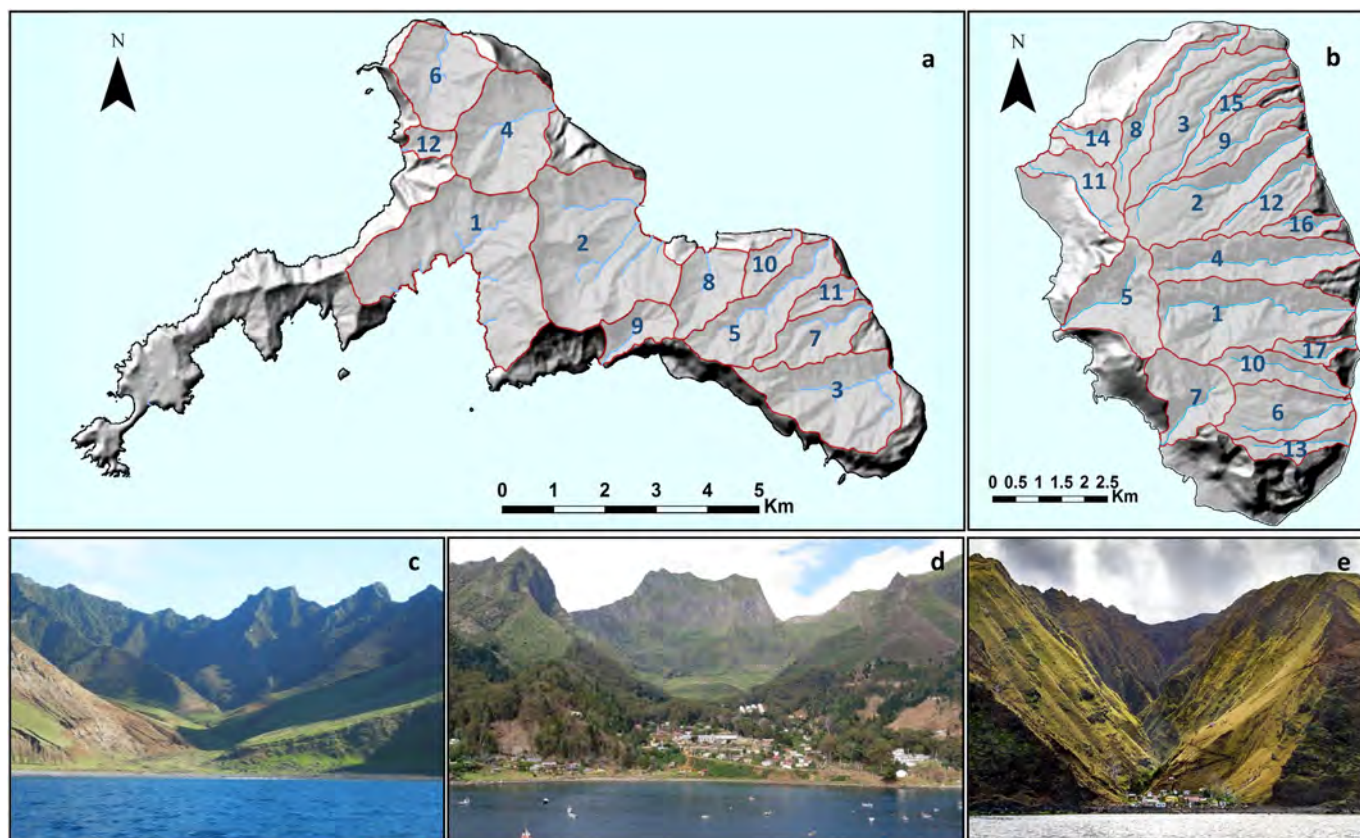


Fig. 7. a) Analysed basins in RC (12); b) and in AS (17); (c) Puerto Inglés basin in RC (ID 4 in Panel a); Cumberland Basin in RC (ID 2 in Panel a); e) Las Casas basin in AS (ID 4 in Panel b). Basins names can be checked in Tables 3 and 5.

The hydrographical system of RC consists of streams that mainly run in a north-easterly direction, forming V-shaped valleys (Fig. 7A). AS presents long and narrow less evolved basins with streams that mainly flow towards the east-northeast (Fig. 7B). Maximum and mean basins slopes are very similar for both islands ranging between 53° – 76° and 21° – 42° , respectively (Table 2). Streams appear normally without permanent water courses the longest one (3.5 km) being on RC (ID 5 Table 3) and a bit longer in AS reaching up to 5 km (ID 4 Table 2). Basins' areas are similar in both islands and range from 0.5 to 6.61 km². Mean basins widths show values between \sim 0.39 km and \sim 2.97 km in RC that are smaller in AS, presenting average widths between \sim 0.29 km and \sim 1.45 km, respectively. Relative widths (W) in RC are mainly high to very high ($W > 0.33$, Table 2). Only one basin (ID 5, Table 2) presents a lower W, indicating a long and narrow watershed. Nevertheless, in AS relative widths are, in their majority low ($W < 0.2$; Table 2), although in this island other basins present very high relative widths mainly corresponding to those basins located at the west of the island (IDs 5, 7, 14 in Table 2; Fig. 7B).

Shape factor (Rf) that relates the basin area with the stream lengths shows low and high evolved basins on both islands, and is directly correlated with their age. Thus, RC presents highly evolved basins with $Rf > 0.25$. There is only one basin with a $Rf < 0.25$ corresponding to ID 5 (Table 2). In the case of AS, higher Rf corresponds to the same basins with high W, indicating they are more evolved than the rest of basins with $Rf < 0.29$. Likewise, those basins with lower Gravelius coefficient (Kc tend to 1) are the least elongated (or more circular) and correspond to the oldest basins, whereas those with $Kc \sim 2$ are the most elongated basins and therefore the youngest ones (Table 2). In this sense, the most circular basins are in RC represented by Puerto Inglés and Vaquería basins (IDs 4, 6; Table 2; Fig. 7A), and AS has developed the most elongated ones (IDs 8, 13, 15; Table 2; Fig. 7B). Other parameters such as basins' maximum heights, perimeter and overall area in % are shown in Table 2.

We used CalHypso ArcGIS Add-in (Pérez-Peña et al., 2009) for extracting the hypsometric curves of twelve drainage basins in RC and seventeen in AS, using the 20 m DEM resolution in both cases. There are clear differences between the curves from the RC and AS Islands (Fig. 8). The curves of AS have very similar, slightly S-shaped forms which are related to a relative maturity stage (Table 3, Fig. 8). Their hypsometric integral (HI) vary between 0.44 and 0.63 being higher than those obtained in RC, that range between 0.29 and 0.6, and then showing that AS basins are in a more youthful stage of development than those of RC (Table 3, Fig. 8). Doña María and Playa Larga basins in AS (IDs 7 and 13; Table 3; Fig. 8), and Corral de Molina, Rabanal y Juanango basins in RC (IDs 9, 10 and 12; Table 3; Fig. 8) present more convex hypsometric curves which are typical of a youthful basin stage, presenting the highest HI values (Table 3, Fig. 8). In RC there is a larger number of concave curves being indicative of a peneplain stage (very eroded), and others with $HI \approx 0.5$, typical of mature or in equilibrium basins (Pérez-Peña et al., 2009 and references therein), being those with lower HI values and then the most eroded basins, Villagra and Cumberland (IDs 1,2 Table 3), located at the centre of the island.

We have also extracted the main statistical moments for the analysed hypsometric curves such as kurtosis (k), skew (s), density kurtosis (dk) and density skewness (ds), that can be interpreted in terms of erosion and basin slope (Table 3). The lower values of skewness correspond to those higher values of HI in both islands (Table 3). In RC those more incised basins present a positive density skew which is indicative of fluvial dominance (Table 3).

4.2.2. Islands paleo-reconstruction

Based on the maximum basin elevations we constructed an artificial reference surface extending contour lines up to closing basins for the first reconstruction method (Fig. 9A, B, C). In this case we assumed minimum paleo-heights and therefore minimum volumes were obtained.

Table 2
Main basins morphological parameters of RC and AS.

ID Map	Island	Name	Orientation	Max./Mean Slope (°)	Max. High H (m)	Perimeter P (km)	Streams Max. Length L (km)	2D Area A (km ²)	% Overall area	Mean width W (km)	Relative width w (W/L)	Shape factor Rf (A/L ²)	Gravellius Coefficient Kc (0.28P/A ^{1/2})	
1	RC	Villagra	SW	75°/30°	912	15.66	1.64	6.61	13.85	2.97	1.81	2.46	1.71	
2		47.77	Cumberland	NE	73°/30°	905	11.31	2.29	6.57	13.76	2.59	1.13	1.25	1.24
3		Km ²	Puerto Francés	ENE	68°/28°	704	9.49	2.52	3.91	8.20	1.35	0.54	0.62	1.34
4			Puerto Inglés	NE	69°/31°	702	7.48	2.28	3.50	7.34	1.52	0.67	0.67	1.12
5			Piedra Agujereada	NE	50°/27°	739	8.75	3.51	2.77	5.81	0.83	0.24	0.23	1.47
6			Vaquería	NE	65°/28°	659	6.54	1.92	2.63	5.51	1.50	0.78	0.71	1.13
7			Pesca de los Viejos	NE	50°/27°	620	6.26	1.56	1.59	3.34	0.63	0.40	0.65	1.39
8			El Pangal	N	64°/34°	738	5.63	1.56	1.67	3.50	0.86	0.55	0.69	1.22
9			Corral de Molina	WSW	68°/39°	720	4.97	1.64	1.00	2.11	0.67	0.41	0.37	1.39
10			Rabanal	NE	60°/22°	461	4.06	0.59	0.72	1.50	0.44	0.74	2.05	1.34
11			Laura	ENE	55°/27°	414	3.61	1.18	0.60	1.26	0.39	0.33	0.43	1.30
12			Juanango	W	56°/38°	603	3.18	0.85	0.50	1.04	0.49	0.57	0.69	1.26
1	AS	Vacas	E	68°/39°	1302	10.96	4.83	5.47	10.22	1.23	0.25	0.23	1.31	
2		53.58	Pasto	NE	63°/29°	1224	10.66	4.69	4.19	7.83	0.96	0.21	0.19	1.46
3		Km ²	Sánchez	NE	59°/22°	1149	11.46	4.71	3.74	6.98	0.68	0.15	0.17	1.66
4			Casas	E	66°/39°	1186	10.86	5.09	3.72	6.94	0.77	0.15	0.14	1.58
5			Lobería Vieja	SW	72°/42°	1314	8.14	2.53	3.06	5.71	1.34	0.53	0.48	1.30
6			Varadero	E	65°/31°	1065	7.50	2.65	2.69	5.02	0.97	0.36	0.38	1.28
7			Playa Larga	SW	77°/40°	1311	7.16	1.94	2.45	4.58	1.45	0.75	0.65	1.28
8			Larga	NE	63°/25°	1165	11.58	4.96	2.18	4.06	0.45	0.09	0.09	2.20
9			Sándalo	NE	56°/25°	931	7.28	2.93	1.77	3.31	0.59	0.20	0.21	1.53
10			Angosta	ESE	67°/34°	1078	7.24	2.92	1.70	3.17	0.57	0.20	0.20	1.55
11			Playa del Buque Varado	NW	72°/34°	1224	7.39	2.55	1.68	3.13	0.68	0.27	0.26	1.60
12			Óvalo	NE	62°/27°	934	6.89	2.51	1.68	3.13	0.60	0.24	0.27	1.49
13			Doña María	E	68°/27°	995	6.93	2.18	0.93	1.74	0.36	0.16	0.20	2.01
14			Imán	NW	69°/41°	1040	4.55	1.19	0.92	1.71	0.63	0.53	0.64	1.33
15			Negra	NE	55°/21°	697	5.44	2.01	0.69	1.30	0.29	0.14	0.17	1.83
16			Mono	E	59°/30°	726	4.22	1.53	0.68	1.27	0.38	0.25	0.29	1.43
17			Inocentes	E	53°/30°	788	4.74	1.74	0.64	1.19	0.34	0.19	0.21	1.66

As a second method, we reconstructed the pre-erosion geometry of a hypothetical conical volcanic edifice using the shelf break as the original 0 m level (Fig. 1) and its centroid as the maximum elevation of the

paleo-island (Fig. 9D–G). Maximum heights reached by the islands in their pre-erosive states using this method yield elevations of ca. 1400 m for AS and 1900 m for RC. Using the empirical Eq. (3), that relates

Table 3
Hypsometric parameters and hypsometric curves of RC and AS basins.

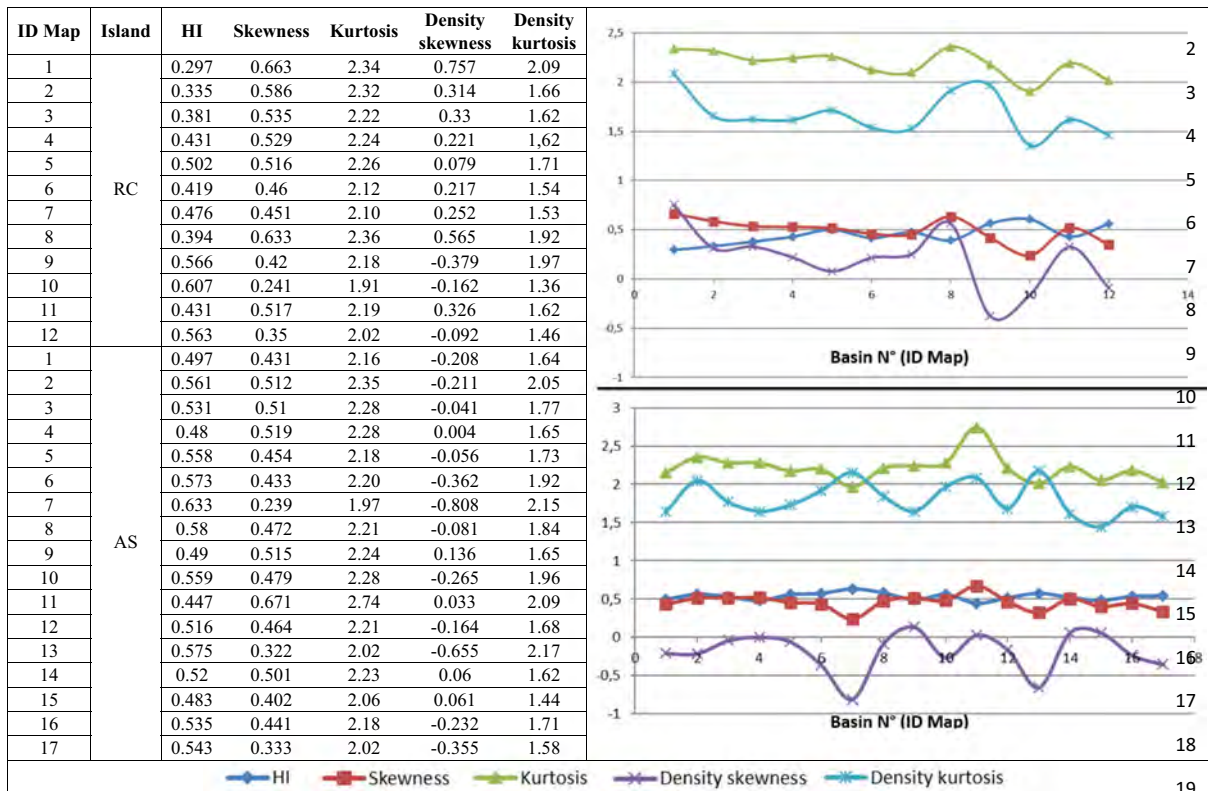


Table 4

Long-term growth rates considering the paleo-islands and the volcano edifices. Growth rates have been estimated without considering erosion neither mass wasting. Subsidence rates are also shown.

	Growth rates			Subsidence rates (mm/yr)
	Volcano edifice (km ³ /Ma)	Paleo-island (km ³ /Ma)	GR island (km ³ /Ma)	
RC	1125.35	109.13	3.15/shield stage 45.33	0.12
AS	1535.18	68.73	30.07	0.19

the maximum island height and the paleo-island area, the estimated elevations are lower reaching 1085 m in AS and 1732 m in RC. Since AS is currently 1372 m high (Table 1), the second method seems to underestimate the former height and therefore we preferred the results from the first method (1400 m – Fig. 9E, F, Table 1). For RC, however, we used the result obtained from the empirical equation since it does not overestimate the volume of the paleo-island (Fig. 9D, F; Table 1).

4.3. Long-term growth and erosion rates

Growth rates were calculated using both the total volume of each volcano edifice (onshore plus offshore volumes considering as level 0 the ocean seafloor) and only considering the paleo-island volume (onshore volume considering as level 0 the shelf break). Thus, we have obtained volumes for the total RC volcano edifice of 6392 km³

and 1658 km³ for AS (Table 1). Considering the maximum inferred age for volcano edifices, which is the age at the bottom of the ocean, for RC (5.68 Ma) and for AS (1.08 Ma) (Table 1), estimated growth rates for the whole volcano edifices are 1125.35 km³/My in RC and 1535.18 km³/My in AS (Table 4). Calculated paleo-island volumes are 472.55 km³ for RC and 64.95 km³ for AS (Fig. 9) and thus related growth rates considering in this case the estimated ages of the shelf breaks (4.33 Ma – RC and 0.945 – AS, Table 1) are only 109.13 km³/My in RC and 68.73 km³/My in AS (Table 4).

We have also estimated volumes associated to the shield and rejuvenated volcanism in RC island. Subaerial shield stage has a residual volume of 12 ± 0.28 km³, the rejuvenated stage representing less than 1 km³. Considering only the emerged parts of the two volcanoes, i.e., the islands with their present volumes and the oldest ages for the exposed sections (Table 1), we obtained even lower growth rates of 3.15 and 30.07 km³/My for RC and AS respectively (Table 4). Since most of the emerged volume of RC has been removed by erosion, being part of this eroded volume deposited offshore (not accounted for the analyses), we have estimated the erosion rates of its paleo-reconstructed shield and rejuvenated stages (Fig. 5). Considering this time the island paleo-reconstructed volume with its base as the current sea level, and the oldest available age for the shield stage in RC (3.95 Ma), we have reconstructed its volume (186 km³) and subtracted the volume occupied by the rejuvenated volcanism (~6 km³), thus obtaining a shield building stage volume of ~180 km³. The estimated growth rate for this stage is 45.3 km³/My. This new data is more in line with the shield stage growth rate obtained for AS Island (30.1 km³/My).

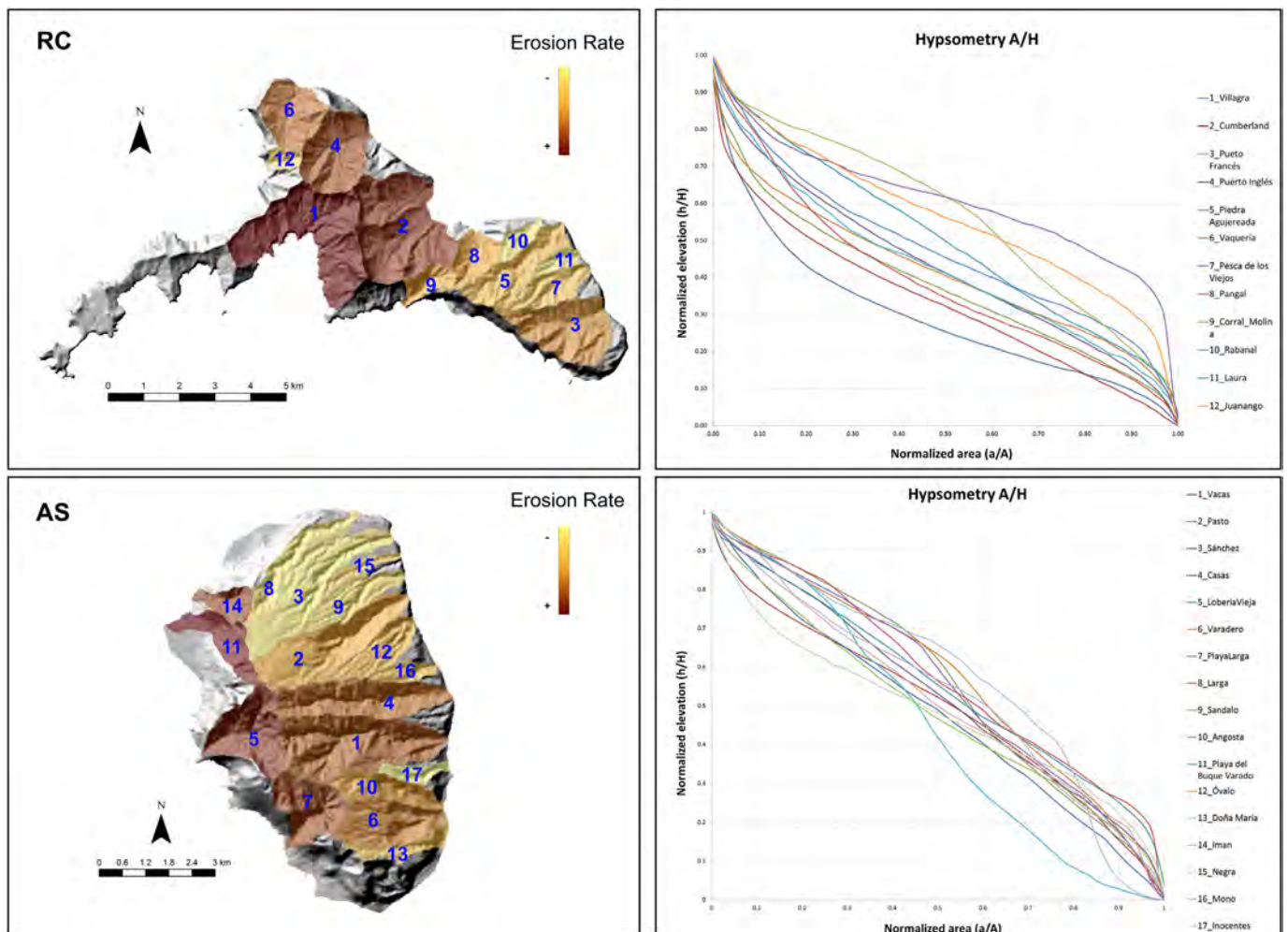


Fig. 8. Erosion rates by basin in RC (a) and AS (b) with its respective hypsometry curves for each of the basin-streams.

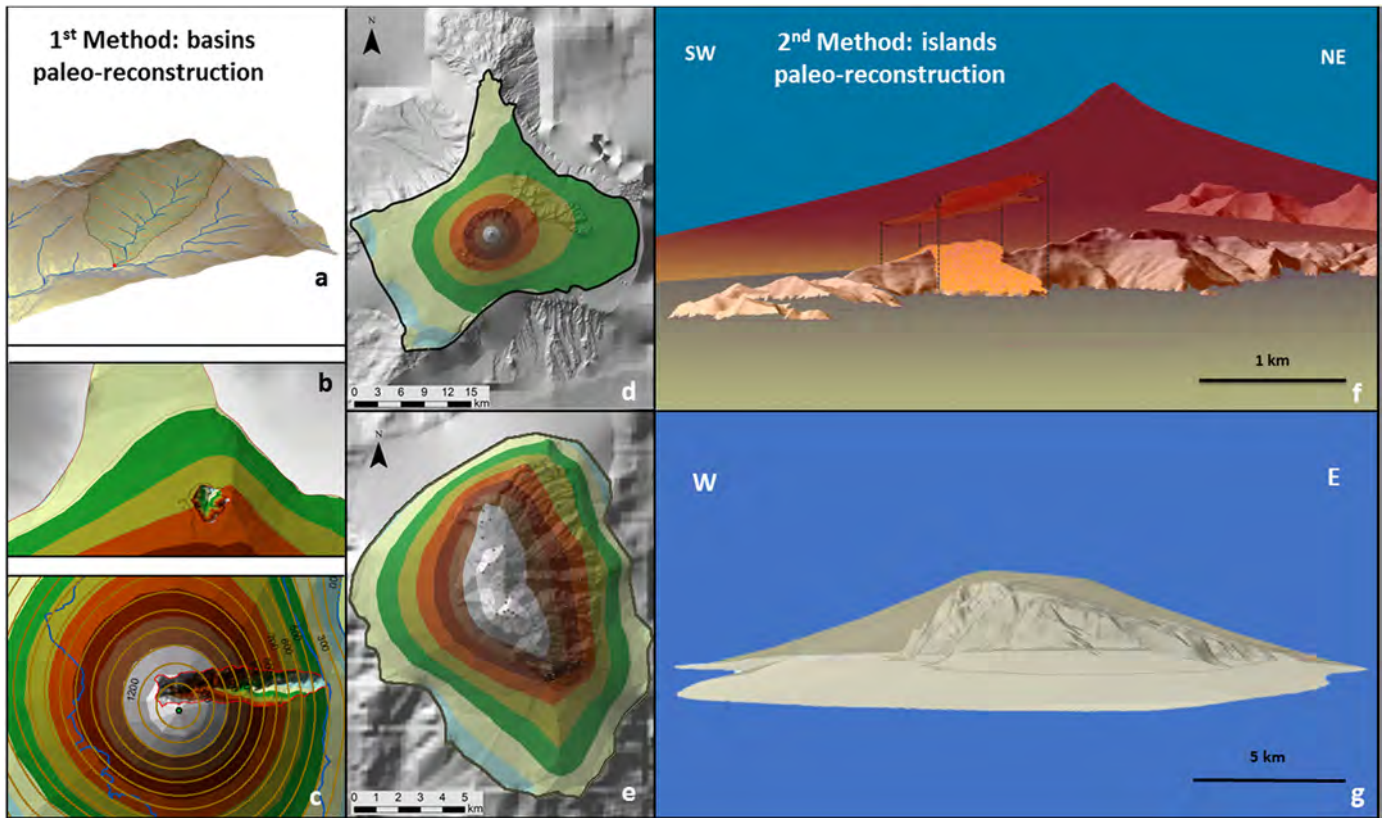


Fig. 9. Volcano-edifice paleo-reconstructions. a–c) Basins paleo-reconstruction method. d–g) Islands paleo-reconstruction method.

4.4. Long-term erosion-rates

According to the paleo-reconstruction method used, either the paleo-basins or the paleo-islands (Fig. 9), we have obtained different values for volumes and therefore for erosion rates (Table 5). Paleo-reconstructions through which we have performed our analyses are shown in Fig. 9. For the first method (paleo-basins reconstruction) we used minimum erosion obtained volumes, while for the second method (paleo-islands reconstruction), this provided maximum eroded volumes. Erosion rates in both cases were computed as the ratio between the corresponding eroded volume (paleo-basin or paleo-island volume) and the age of the youngest volcanic activity of each basin. We used the ages of the head of each basin in RC that range between 3.95 Ma and 3.75 Ma, and 0.83 Ma for AS (Table 5; Fig. 9A–C).

Calculated eroded volumes for the twelve RC basins make a total of 7.39 km³ whereas the seventeen basins of AS reach 6.75 km³ (Table 5). Individually, these eroded volumes range from 2.21 km³ for Villagra basin to 0.02 km³ for Rabanal in RC (Table 5). Eroded individual basin volumes in AS range from 1.53 km³ (Lobería Vieja) to 0.03 km³ (Negra and Inocentes basins) (Table 5). In terms of erosion rates these values represent an average of 0.16 km³/My and 0.49 km³/My for RC and AS, respectively (Table 5). Values for each basin are given in different units (km³/My m/My and t/km²yr) in Table 5. We have used a mean density of 3 g/cm³ for the representative volcanic rocks forming the islands to calculate erosion rates in t/km²yr (Table 5).

Considering the data obtained through the paleo-island reconstruction method (grey columns in Table 5), the calculated eroded volumes sum a total of 14.43 km³ for RC and 6.97 km³ for AS. Individual basin values range from 4.91 km³ to 0.12 km³ in RC corresponding also to Villagra and Rabanal basins (Table 5). AS presents more similar values than those obtained with the first method, ranging from 1.49 km³ to 0.03 km³ (Table 5). Regarding the erosion rates, in RC these are up to three times higher than those obtained with

the first method, and results from both methods are very similar in AS. Thus, average erosion rates in RC reaches 0.31 km³/My and 0.50 km³/My in AS (Table 5).

Area–erosion rates relationships for basins display a positive correlation with the degree of erosion in both islands, especially in RC. The wider and secondly the longer basin, the more erosion rates they present (Fig. 8A, B; Table 5). Correlation coefficients (R^2) for areas vs erosion rates are 0.94 in RC and 0.87 in AS. The latter has been obtained only considering the basins located at the east of the island since the whole basins displayed a low R^2 of 0.5.

5. Discussion

5.1. Uncertainty of the geomorphological approach

The current landscape of RC and AS islands is the result of long-term erosive processes that compete with growth mechanisms during the shield stage and dominate in the post-shield stage that are currently dismantling their volcanic landforms. It is important to note that these islands represent only a small fraction of the total volcano edifices. RC island represents the 0.2% of the total volcano edifice, while AS the 1.55%. This is not unusual in oceanic islands. For example, Stromboli has an emerged part that represents only 2% of the total volume (Casalbore, 2018), and Ascension Island includes a subaerial sector that accounts for only 1% of its total volume (Harris, 1983). This fact implies that our understanding of subaerial processes is extrapolated to the submarine section, which limits the extent of the results.

The methodological approach here presented is based on paleo-reconstructions, and in the case of RC should be considered only as a first order, since the island is highly incised and any reconstruction, considering the degree of erosion of this island edifice is rough approximation that might not be accurate. Nevertheless, the two methods used provide minimum and maximum volumes and subsequently growth and erosion

Table 5
Total and averaged erosion rates calculated using the two paleo reconstruction methods described in the text and following Eqs. (5)–(7).

ID Map	Island	Name	3D Area (km ²)	Age (Ma)	Eroded Volume Paleo Basins (km ³)	Eroded Volume Paleo Island (km ³)	Erosion Rates Paleo Basins (km ³ /Ma)	Erosion Rates Paleo Island (km ³ /Ma)	Erosion Rates Paleo Basins (m/Ma)	Erosion Rates Paleo Island (m/Ma)	Erosion Rates Paleo Basins (t/km ² yr)	Erosion Rates Paleo Island (t/km ² yr)
1	RC	Villagra	8.40	3.87	2.21	4.91	0.57	1.27	69.82	151.11	209.47	453.34
2		Cumberland	7.86	3.89	2.05	3.42	0.53	0.88	66.53	111.72	199.59	335.18
3		Puerto Francés	4.48	3.81	0.64	1.40	0.17	0.37	38.12	82.24	114.35	246.73
4		Puerto Inglés	4.20	3.75	0.83	1.51	0.22	0.40	52.91	95.81	158.74	287.45
5		Piedra Agujereada	3.04	3.81	0.21	0.64	0.06	0.17	18.28	55.22	54.84	165.67
6		Vaqueria	2.93	3.75	0.69	0.70	0.19	0.19	57.49	63.63	172.48	190.90
7		Pesca de los Viejos	1.71	3.81	0.10	0.39	0.03	0.10	15.41	60.35	46.22	181.05
8		El Pangal	1.80	3.95	0.26	0.58	0.07	0.15	39.85	82.22	119.55	246.65
9		Corral de Molina	1.31	3.95	0.27	0.46	0.07	0.12	20.85	89.2	152.45	267.60
10		Rabanal	0.71	3.81	0.02	0.12	0.01	0.03	9.08	45.95	27.25	137.87
11		Laura	0.63	3.81	0.03	0.14	0.01	0.04	14.22	60.11	42.67	180.35
12		Juanango	0.61	3.87	0.08	0.16	0.02	0.04	34.56	69.51	103.70	208.54
Total/Average		-	37.68/3.14	-	7.39/0.61	14.43/1.20	1.95/0.16	3.76/0.31	437.12/36.42	967.07/80.58	1401.31/116.77	2901.33/241.77
1	AS	Vacas	7.43	0.83	1.12	1.10	1.35	1.32	181.65	177.94	545.27	533.81
2		Pasto	4.89		0.44	0.57	0.53	0.69	108.01	140.81	324.04	422.42
3		Sánchez	3.97		0.17	0.28	0.21	0.34	53.04	85.29	159.13	255.88
4		Casas	4.80		0.60	0.66	0.73	0.80	151.74	166.49	455.22	499.47
5		Lobería Vieja	4.40		1.53	1.49	1.85	1.80	420.11	409.90	1260.33	1229.70
6		Varadero	3.14		0.34	0.39	0.41	0.48	131.84	151.62	395.53	454.86
7		Playa Larga	3.45		0.80	0.83	0.96	1.00	278.46	289.91	835.39	869.73
8		Larga	2.36		0.11	0.18	0.13	0.22	55.73	94.19	167.19	282.56
9		Sándalo	1.86		0.09	0.10	0.10	0.12	55.79	64.08	167.36	192.24
10		Angosta	2.05		0.21	0.23	0.26	0.28	125.15	135.60	375.45	406.81
11		Playa Buque Varado	2.12		0.74	0.59	0.90	0.72	424.03	338.29	1272.10	1014.86
12		Óvalo	1.82		0.11	0.09	0.13	0.10	72.15	57.27	216.46	171.82
13		Doña María	0.94		0.05	0.07	0.06	0.09	63.16	97.35	189.49	292.04
14		Imán	1.20		0.34	0.29	0.41	0.35	339.49	295.41	1018.48	886.22
15		Negra	0.67		0.03	0.03	0.04	0.04	57.09	55.27	171.27	165.82
16		Mono	0.72		0.04	0.04	0.05	0.05	72.17	76.07	216.51	228.21
17		Inocentes	0.64		0.03	0.03	0.03	0.04	48.57	69.12	148.60	207.36
Total/Average		-	46.46/2.73	-	6.75/0.39	6.97/0.41	8.15/0.49	8.44/0.50	2638.18/155.18	2704.61/159.09	7917.82/465.75	8113.81/477.28

rates, providing a range of values from what an implicit uncertainty might be derived. In addition, paleo-reconstruction methods used in the literature have only considered the present sea level as the subaerial base of the studied volcano (e.g. Ricci et al., 2015; Hildenbrand et al., 2008). In this study we have used the uppermost shelf break position of the volcano edifice as the base for one of our paleo-reconstruction, and the sea bottom for the other one, since we considered these as the most accurate way to study the whole paleo-island and volcano-edifice. We denote that sometimes the shelf break does not necessarily represents the subaerial/submarine slope break of the original volcano, generally resulting from a combination of erosion, glacio-eustatic oscillations and subsidence/uplift. Onshore published ages have been used to infer the insular shelf and the edifice age at the seafloor. A more complete age catalogue with some submarine tie points would be useful to better constrain the age and therefore to reduce the uncertainties of the estimations.

Erosion Rates calculated through basins paleo-reconstruction represent minimum rates since we have only created a reference surface that closes the current basins. Those calculated using a conical pre-erosion volcano as a proto-island and the identified shelf breaks as basis are considered as maximum erosion rates. On the other hand, mass wasting, coastal and chemical erosion are not specifically computed in this study and they can be the responsible of a part of the non-computed erosion. Therefore, volumes and erosion rates could have been underestimated.

Regarding DEMs used, the combined bathymetrical DEM was created through the combination of different resolution information. Unfortunately, all the available bathymetric maps do not have high enough resolution neither a complete coverage to distinguish accurate shelf-breaks or any other submarine structure (e.g. more landslide scars or mass wasting deposits, submarine channels, etc.) and therefore to delimit the summit plateau area with absolute precision. A more complete and comprehensive bathymetry is required to avoid skewed terrain interpretations. The topographical map used (20 m resolution)

however, is complete and represents well but not identically the terrain surface, presenting an implicit discrepancy between the model and the real highs, areas and volumes calculated. Nonetheless, these discrepancies, between the real heights and those represented by the DEM represent less than 0.5% according to the metadata provided by SAF.

5.2. Submarine markers of vertical movements

The depth and morphological features of RC and AS insular shelves suggest they are the result of active marine erosion during mostly the Quaternary glacio-eustatic oscillations and subsidence that could have been interrupted by uplift periods reflected in the position of emerged marine sediments (Sepúlveda et al., 2015). A first order of subsidence rates can be estimated using the current position of the shelf breaks (−510 m at RC and −175 m at AS) and their estimated ages (4.33 Ma - RC; 0.945 Ma - AS). Thus, we have obtained subsidence rates of ~0.12 mm/yr for RC and ~0.19 mm/yr for AS (Table 4). This long-term subsidence could be related to the flexural loading of the lithosphere, to the lithosphere cooling processes and/or by hotspot drift or hotspot swell decay (Ramalho et al., 2013 and references therein). Moore (1987) and Huppert et al. (2015) observed in Hawaii that subsidence rates decrease with time, being higher during the first million years. Our results also demonstrate this hypothesis were the younger AS island presents higher subsidence rates than the older RC. Islands as Kaua'i have experienced a mean subsidence rate of 0.45 mm/yr in the period from ~3.9 to ~1.7 Ma (Thordarson and García, 2018). This rate is slow and is of the same order of magnitude than our islands values comparing with the subsidence rates average for the whole Hawaiian archipelago (~2 mm/yr according to Table 1 of Huppert et al., 2015). Average subsidence rates for São Jorge and Faial in the Azores are in the same range than our results being >0.11 mm/yr and >0.17 mm/yr, respectively (Quartau et al., 2018). Tahiti and La Gomera (Canary Islands) also present similar long-

term average rates (0.25 mm/yr; Thomas et al., 2012 and references therein; Izquierdo et al., 2013).

The absence of identified terraces on the shelves may be firstly related to the lack of a complete high-resolution bathymetry coverage that does not allow to identify them or also to sediment infilling of the space created by earlier erosion as it was suggested by Quartau et al. (2010) in Faial Island (Azores, Portugal). These shelves' terraces are the markers of vertical movements that volcanic edifices have experienced along their geological lives. Considering the long-term average rates of shelf widening, Menard (1983, 1986) reported that insular shelves widen initially at rates of 0.6 to 1.7 mm/yr, (0.6 mm/yr for the Canaries; 1.1 mm/yr for Hawaii; 1.7 mm/yr for the Marquesas). Similar widening rates were calculated by Dickson (2004) for Lord Howe Island (1.7 mm/yr). Our results for RC and AS that range from 3.35 to 5.05 mm/yr, respectively, are more in accordance with those proposed by Le Friant et al. (2004) for Monserrat (3.8–5.5 mm/yr), or by Quartau et al. (2010) for Faial Island (2–7 mm/yr) obtained from the oldest shelf sectors. RC, the oldest island (ca. 4 Ma), presents lower enlargement rates than AS (ca. 1 Ma), which agrees with the conclusion proposed by previous authors (e.g., Menard, 1983, 1986; Trenhaile, 2000; Quartau et al., 2010) that widening rates decrease through time. As a local signature, the widest shelves areas on both islands are related to the south-west wind direction. Subsidence has been recognised as having an important role on shelf generation and development, higher widening values here obtained for both islands and especially in AS could be related to the aforementioned subsidence process.

5.3. Factors that control the growth and decay of volcanic oceanic islands

Beyond the inherent uncertainties, estimated volumes and growth rates considering the total volcano edifice (VE) and the paleo-island (PI) yield different results. RC volcano edifice is almost four times bigger in terms of volume than AS volcano edifice (6392 km³ vs 1658 km³ – Table 1) whereas is 7.27 times bigger if we only consider the paleo-islands volumes (472.55 km³ vs 64.95 km³ – Table 1). Regarding the volumes obtained for the remaining emerged parts of the volcanoes, AS is almost double in terms of volume than RC (28.27 km³ vs 12.93 km³ – Table 1). Since RC Island is older than AS, the erosion processes have acted during more time dismantling more volume of material. Despite the age, contrasting volumes would imply different melting rates in the mantle plume, which in turn could be related to temperature of the plume and the strength of the oceanic lithosphere (e.g., Lara et al., 2018). These perhaps relevant differences are masked here in the calculus when we consider the remaining island, the paleo-island or the volcanic edifice as a whole.

Despite the estimated volcano edifice volume for RC being larger than the one AS, calculated growth rates are similar for both volcanoes, yielding a value between ~1125 and ~1545 km³/My. Nevertheless, growth rates only considering the paleo-islands are larger for RC (~109 km³/My) than for AS (~69 km³/My) (Table 1).

In the literature we commonly find volumes or growth rates estimated only for the emerged part of the edifice or related to certain volcanoes or stages of the volcanic island (e.g. White et al., 2006), data that is obtained depending on the set of geochronological data for each location and considering the current remaining volumes of the islands. This fact makes difficult to compare the obtained volumes or growth rates between the different settings since commonly growth rates are estimated without considering the erosion volumes. This stresses the need to reconstruct paleo-islands volumes or to consider the total volcano edifice volumes in order to obtain more reliable growth rates.

Our growth rates calculated for the reconstructed shield-building stage of RC are on the same order of magnitude as the ones for other hotspot volcanoes (between ~30–45 km³/My). This is the case of Bouvet Island (Norway), Santo Antão (Cape Verde), Ascension Island or El Hierro (Canary Islands) that show growth rates between 40 and 85

km³/My, calculated for the last 0.7 Ma, 1.75 Ma, 1.5 Ma and 1.12 Ma, respectively (Gerlach, 1990; Plesner et al., 2003; White et al., 2006; Becerril, 2014). The growth rate obtained from the remaining volumes of the island gives much lower values, even an order of magnitude less than the rates obtained for the paleo-shield reconstruction (RC: 3.15 km³/My). Construction rates calculated for other geodynamic contexts such as some of the Lesser Antilles (Dominica Island, Saba and Grenada islands) present growth rates between 15 and 400 km³/My (Wadge, 1984; Ricci et al., 2015) that are in agreement with our results, although processes involved have different sources related to arc-volcanism in the Lesser Antilles. Volumes and growth rates calculated for Hawaiian individual shield volcanoes and islands are instead much larger (even two orders of magnitude) than those obtained for Juan Fernández (e.g., Robinson and Eakins, 2006 and references therein), which describe the effect of a large-scale swell underneath but perhaps also the difference of taking individual volcanic succession or integrated paleo edifices on long-term estimations and probably due to a larger availability of radiometric ages for Hawaiian archipelago than other islands.

The total maximum removed material in RC (14.43 km³) only represents 3% of the total bulk volume of the paleo-island, while the total minimum (7.39 km³) represents 1.5% of the total bulk volume but around 57% of its subaerial volume (12.93 km³). Regarding total erosion rates calculated by paleo-island method in RC, values are less than half (3.76 km³/My) than those obtained in AS (8.44 km³/My) and four times less (1.95 vs. 8.15 km³/My) than those calculated by the paleo-basins method (Table 5).

RC presents lower total and averaged erosion rates than AS which can be explained by an erosion rate decreasing through time where streams have reached their equilibrium profile in the oldest island. This is also supported by the hypsometric integral (HI) results for RC, where more than half of the basins show HI ~ 0.5. Some basins in RC have major erosion rates than others, which could be the response to the longer erosive history related to older materials (shield stage materials). Small drainage basins (mainly those at the east mostly related to rejuvenated volcanism, Fig. 9) show fewer erosion rates that we assign to a shorter erosive history. Western basins in AS have not only a different morphology than the eastern ones, they also present greater erosion rates. These basins could have been severely affected by large landslides, which shaped and widen their headwaters. However, landslides seem not to be a widespread process in the eastern sector of the island where the basins form deep and narrow gullies. Other archipelagos such as the Canary Islands have been eroded and dismantled by recurrent landslides that played an important role in shaping the islands' geomorphology (e.g., Carracedo, 1999; Acosta et al., 2005; Menéndez et al., 2008). Nevertheless, intense onshore erosion may be the responsible of remobilisation of any remnant of massive landslides in JF, which could be only inferred from the roughness of the ocean floor at the foot of the slope around the edifices (Figs. 5; A.1).

If the erosion rates are maintained over time, the islands could be completely dismantled in the next 8–10 Ma (without considering the vertical movements that they experience by isostasy, neither the contribution of coastal erosion). It is important to note that we have not considered the possible vertical movements that the islands have experienced. We have only calculated subsidence rates considering the current shelf break positions and their ages.

We have also compared erosion rates of other volcanic settings with similar ages than RC and AS, which present basin-average erosion rates of 116.77 and 465.75 in t/km²yr, respectively. Erosion rates calculated for Hawaii range from 110 to 500 t/km²yr (Li, 1988). In the particular case of Kaua'i, basin-averaged erosion rates over the past ~5 Ma are highly variable in space, ranging from 8 to 335 t/km²yr (Ferrier et al., 2013). São Miguel in the Azores (Portugal – 4 Ma), presents mechanical erosion rates for basins of 170–500 t/km²yr (Louvat and Allègre, 1998). These results are in the same range than those obtained for Juan Fernández islands, however these settings present higher and sometimes two-fold annual

average precipitation rates than in RC and AS (JF: 973 mm; Kau'I: 2256 mm; São Miguel: 2400 mm).

The latter implies that high erosion rates in JF are at least partially controlled by factors other than mean annual precipitation. With the exception of Hawaii, most of the reported subsidence rates in oceanic islands are comparable and thus subsidence could be a factor that is favouring erosion but not the dominant cause. On the other hand, hypsometrical curves do not indicate significant uplift processes, despite the abnormal value reported for last millennia in Robinson Crusoe (~8.5 mm/yr - Sepúlveda et al., 2015), which could be reinterpreted. New research focused on identifying paleo-markers would help to decipher if uplift might be playing a role on the islands dismantling.

Observing the emerged parts of the islands, coastal erosion could also play a fundamental role in rapidly dismantling them since they are characterised by active cliffs that reach up to 1000 m from sea level, being the most active cliffs those located at the south of the islands (windwards). Most of basins in RC present headwaters with exception to those located to the east, which have been probably removed by coastal erosion (Fig. 7A). In AS those the western basins are probably the product of large landslides that have contributed to widen them (Fig. 7B). These two processes, coastal erosion and mass wasting, could be pivotal in removing high volumes and therefore they could play a fundamental role on comparatively higher erosion rates associated with lower annual rainfall rates when compared with other oceanic settings. Nevertheless, this requires a detailed analysis to discriminate the volumes that have been removed by landscape processes from those eroded by coastal and marine erosion.

Other processes, directly related to the above mentioned, such as wind direction and intensity effects or the orographic precipitation effect could also result in erosion asymmetries on the islands. Higher cliffs and hanging basins on RC and AS appear windward meanwhile those basins less dissected that flow into the sea are located leeward. On the other hand, precipitation on the islands is unevenly distributed due to orographic effects. Rainfall sometimes induce torrential regime to fluvial erosion on the north and east slopes associated with short but heavy downpours.

6. Conclusions

The present study is based on quantitative bathymetric and topographical analyses complemented with field investigations of the only two emerged volcanoes of the JFR: Robinson Crusoe and Alejandro Selkirk Islands. This research allowed us to identify geomorphological features both offshore and onshore that have been the base to perform paleo-reconstructions and to understand the geomorphological evolution of these volcanoes. The main conclusions obtained are listed below:

- From the submarine analysis performed we observe that the depth and morphological features of the RC and AS insular shelves suggest they are the result of active marine erosion. The insular platform of RC is more extensive than the AS one, indicating a more advanced state of erosion. Nevertheless, RC, older in age, presents fewer shelf enlargement rates than AS which indicates these rates decrease over time. Likewise, long-term subsidence rates estimated from the shelf break depth also decrease with time being higher during the first million years of islands life. Our results demonstrate the hypothesis of time-decreasing subsidence rates stated by Moore (1987) and Huppert et al. (2015).
- Growth rates calculated for the reconstructed shield-building stage of RC and AS are in the same order of magnitude than other obtained in similar geodynamic contexts. Contrary to just considering the remaining emerged parts of the edifices, these results reveal the need to attempt a fully reconstruction of paleo-islands or to consider the total volcano edifice volumes when emerged parts are intensely eroded, thus aiming for more accurate growth rates estimations.

- Our study shows that despite erosion rates in RC and AS range in the same order of magnitude when compared to other volcanic islands such as Tahiti, Azores or Hawaii, they would be rather higher when a smaller rainfall regime is considered. The mechanism playing a role on these high erosion rates could be related to vertical movements, hence causative of exhumation, or to a combined action of tectonics, coastal and mass wasting processes.

The results of this study also show the importance of field and marine integrated studies and how relevant ocean volcanoes paleo-reconstructions are to unravel the geological and geomorphological evolution of ocean volcano edifices. As it was already denoted by Ferrier et al. (2013), to know which factors determine the ocean volcano islands landscape evolution over time and space is still an open challenge. This study also opens new questions about the causes that influence the geomorphological evolution of oceanic islands. In fact, to determine the role of short term erosion-rates, coastal erosion, vertical movements or mass wasting processes on the evolution of Juan Fernández Archipelago require a future detailed analysis.

Declaration of competing interest

The authors declare that they have no known competing financial interests or personal relationships that could have appeared to influence the work reported in this paper.

Acknowledgements

This research was funded by Agencia Nacional de Investigación y Desarrollo (ANID, Chile) (Fondecyt Postdoctoral grant 3180257 awarded to LB and Fondecyt 1141303 to LEL). We are very grateful to CONAF for all the support given during fieldtrips. We specially would like to thank Felipe Paredes for his invaluable help guiding us through the inaccessible areas of the islands. The first author also thanks to Fundación Endémica for managing the Alejandro Selkirk scientific expedition 2020, and also to the local community for its invaluable support. High resolution multibeam bathymetry was provided by FIPA 2014-04-1 project (Juan Díaz-Naveas) and by CIMAR 22 (Cristian Rodrigo), obtained during two cruises of AGS 61 Cabo de Hornos vessel in 2014 and 2016. BENTOS Company provided high-resolution bathymetry of the Cumberland bay in Robinson Crusoe Island.

We are very grateful to R. Ramalho and the other anonym reviewer since they have provided constructive criticism that helped to improve the final manuscript.

Appendix A. Supplementary data

Supplementary data to this article can be found online at <https://doi.org/10.1016/j.geomorph.2020.107513>.

References

- Acosta, J., Uchupi, E., Muñoz, A., Herranz, P., Palomo, C., Ballesteros, M., ZEE Working Group, 2005. Geologic evolution of the Canarian Islands of Lanzarote, Fuerteventura, Gran Canaria and La Gomera and comparison of landslides at these islands with those at Tenerife, La Palma and El Hierro. *Geophysics of the Canary Islands*. Springer, Dordrecht, pp. 1–40.
- Astudillo, V., 2014. Geomorfología y evolución geológica de la isla Robinson Crusoe, archipiélago Juan Fernández. Memoria para optar al título de geólogo. Universidad de Chile, Facultad de Ciencias Físicas y Matemáticas, Santiago (144 pp).
- Baker, P.E., 1967. An outline of the geology of the Juan Fernandez Archipelago. *Geol. Mag.* 104 (2), 110–115.
- Baker, P.E., Gledhill, A., Harvey, P.K., Hawkesworth, C.J., 1987. Geochemical evolution of the Juan Fernandez Islands, SE Pacific. *J. Geol. Soc. Lond.* 144, 933–944.
- Becerril, L., 2014. Volcano-structural Study and Long-term Volcanic Hazard Assessment on El Hierro Island (Canary Islands). (Doctoral dissertation, Ph. D. Thesis). University of Zaragoza, Spain.
- Booker, J., Bullard, E.C., Grasty, R.L., 1967. Paleomagnetism and age of rocks from Easter island and Juan Fernandez. *Geophys. J. R. Astron. Soc.* 12 (59), 469–471.

- Carracedo, J.C., 1999. Growth, structure, instability and collapse of Canarian volcanoes and comparisons with Hawaiian volcanoes. *J. Volcanol. Geotherm. Res.* 94 (1), 1–19.
- Carter, A., van Wyk de Vries, B., Kelfoun, K., Bachèlyre, P., Briole, P., 2007. Pits, rifts and slumps: the summit structure of Piton de la Fournaise. *Bull. Volcanol.* 69, 741–756.
- Casalbore, D., 2018. Volcanic islands and seamounts. *Submarine Geomorphology*. Springer, Cham, pp. 333–347.
- Chadwick, W.W., Howard, K.A., 1991. The pattern of circumferential and radial eruptive fissures on the volcanoes of Fernandina and Isabela islands, Galapagos. *Bull. Volcanol.* 53, 259–275.
- Chen, Y.C., Sung, Q.C., Cheng, K.Y., 2003. Along-strike variations of morphotectonic features in the Western Foothills of Taiwan: tectonic implications based on stream-gradient and hypsometric analysis. *Geomorphology* 56 (1–2), 109–137.
- Clague, D.A., Dixon, J.E., 2000. Extrinsic controls on the evolution of Hawaiian ocean island volcanoes. *Geochem. Geophys. Geosyst.* 1 (4).
- Courtillot, V., Davaille, A., Besse, J., Stock, J., 2003. Three distinct types of hotspots I the Earth's mantle. *Earth Planet. Sci. Lett.* 205, 295–308. [https://doi.org/10.1016/S0012-821X\(02\)01048-8](https://doi.org/10.1016/S0012-821X(02)01048-8).
- Decker, R.W., 1987. Dynamics of Hawaiian volcanoes: an overview. *US Geol. Surv. Prof. Pap.* 1350, 997–1018.
- Dickson, M.E., 2004. The development of talus slopes around Lord Howe Island and implications for the history of island planation. *Aust. Geogr.* 35 (2), 223–238.
- Farley, K.A., Basu, A.R., Craig, H., 1993. He, Sr and Nd isotopic variations in lavas from the Juan Fernandez Archipelago, SE Pacific. *Contrib. Mineral. Petrol.* 115, 75–87. <https://doi.org/10.1007/BF00712980>.
- Ferrier, K.L., Perron, J.T., Mukhopadhyay, S., Rosener, M., Stock, J.D., Huppert, K.L., Slosberg, M., 2013. Covariation of climate and long-term erosion rates across a steep rainfall gradient on the Hawaiian island of Kaua'i. *Bulletin* 125 (7–8), 1146–1163.
- Gerlach, D.C., 1990. Eruption rates and isotopic systematics of ocean islands: further evidence for small-scale heterogeneity in the upper mantle. *Tectonophysics* 172 (3–4), 273–289.
- Gerlach, D.C., Hart, S.R., Morales, V.W.J., Palacios, C., 1986. Mantle heterogeneity beneath the Nazca plate: San Felix and Juan Fernandez islands. *Nature* 322, 165–169. <https://doi.org/10.1038/322165a0>.
- Germa, A., Quidelleur, X., Labanieh, S., Lahitte, P., Chauvel, C., 2010. The eruptive history of Morne Jacob volcano (Martinique Island, French West Indies): geochronology, geomorphology and geochemistry of the earliest volcanism in the recent Lesser Antilles arc. *J. Volcanol. Geotherm. Res.* 198 (3–4), 297–310.
- Gil, C., 2003. Bibliografía sobre el Archipiélago de Juan Fernández, reserva de la biosfera de Chile. *Gestión Ambiental* 9, 79–103.
- Harlin, J.M., 1978. Statistical moments of the hypsometric curve and its density function. *J. Int. Assoc. Math. Geol.* 10 (1), 59–72.
- Harris, C., 1983. The petrology of lavas and associated plutonic inclusions of Ascension Island. *J. Petrol.* 24, 424–470.
- Hedge, C.E., 1978. Strontium isotopes in basalts from the Pacific Ocean Basin. *Earth Planet. Sci. Lett.* 38, 88–94.
- Hildenbrand, A., Gillot, P.-Y., Marlin, C., 2008. Geomorphological study of long-term erosion on a tropical volcanic ocean island: Tahiti-Nui (French Polynesia). *Geomorphology* 93, 460–481.
- Huppert, K.L., Royden, L.H., Perron, J.T., 2015. Dominant influence of volcanic loading on vertical motions of the Hawaiian Islands. *Earth Planet. Sci. Lett.* 418, 149–171.
- Hurtrez, J.E., Lucazeau, F., 1999. Lithological control on relief and hypsometry in the Hérault drainage basin (France). *Comptes Rendus de l'Académie des Sciences-Series IIA-Earth and Planetary Science* 328 (10), 687–694.
- Hutchinson, M.F., Gallant, J.C., 1999. Representation of terrain. In: Maguire, D.J., Goodchild, M.F., Rhind, D., Longley, P. (Eds.), *Geographical Information Systems: Principles, Technical Issues, Management Issues and Applications*. Geoinformation International, pp. 105–124.
- IREN, 1982. Estudio de los recursos físicos Archipiélago Juan Fernández. (Inf. IREN N.45/1982).
- Izquierdo, T., Abad, M., Rodríguez-Vidal, J., 2013. Geomorphological Evidence of Drowned Marine Shelves: A Review of the Offshore Data for la Gomera Island (Canary Islands). *V RCANS CONGRESS*, Huelva, Spain.
- Lara, L.E., Reyes, J., Piña-Gauthier, M., Orozco, G., 2013. Geological evidence of a post shield stage at the Juan Fernandez Ridge, Nazca Plate. *IAVCEI 2013 Scientific Assembly Abstracts*, 20–24 July, Kagoshima, Japan.
- Lara, L.E., Reyes, J., Diaz-Naveas, J., 2018. ⁴⁰Ar/³⁹Ar constraints on the age progression along the Juan Fernández Ridge, SE Pacific. *Front. Earth Sci.* 6, 194.
- Lara, L.E., Moreno, R., Valdivia, V., Aránguiz, R., Lagos, M., 2020. The AD1835 eruption at Robinson Crusoe Island discredited: geological and historical evidence. *Progress in Physical Geography: Earth and Environment*, 030913320937998.
- Le Friant, A., Harford, C.L., Deplus, C., Boudon, G., Sparks, R.S.J., Herd, R.A., Komorowski, J.C., 2004. Geomorphological evolution of Montserrat (West Indies): importance of flank collapse and erosional processes. *J. Geol. Soc.* 161 (1), 147–160.
- Li, Y.H., 1988. Denudation rates of the Hawaiian Islands by rivers and groundwaters. *Pacific Science*. 42. University of Hawaii Press, pp. 3–4.
- Lifton, N.A., Chase, C.G., 1992. Tectonic, climatic and lithologic influences on landscape fractal dimension and hypsometry: implications for landscape evolution in the San Gabriel Mountains, California. *Geomorphology* 5 (1–2), 77–114.
- Louvat, P., Allègre, C.J., 1998. Riverine erosion rates on São Miguel volcanic island, Azores archipelago. *Chem. Geol.* 148 (3–4), 177–200.
- Luebert, F., Plissock, P., 2012. Variabilidad climática y bioclimas de la Región de Valparaíso, Chile. *Investig. Geogr. Chile* 44, 41–56 (2012).
- Luo, W., 2000. Quantifying groundwater-sapping landforms with a hypsometric technique. *Journal of Geophysical Research: Planets* 105 (E1), 1685–1694.
- Luo, W., 2002. Hypsometric analysis of Margaritifer Sinus and origin of valley networks. *Journal of Geophysical Research: Planets* 107 (E10), 1.
- Menard, H.W., 1983. Insular erosion, isostasy, and subsidence. *Science* 220, 913–918.
- Menard, H.W., 1986. *Islands*. Scientific American Library.
- Menéndez, I., Silva, P.G., Martín-Betancor, M., Pérez-Torrado, F.J., Guillou, H., Scaillet, S., 2008. Fluvial dissection, isostatic uplift and geomorphological evolution of volcanic islands (Gran Canaria, Canary Islands, Spain). *Geomorphology* 102, 189–203. <https://doi.org/10.1016/j.geomorph.2007.06.022>.
- Mitchell, N.C., 2001. The transition from circular to stellate forms of submarine volcanoes. *J. Geophys. Res.* 106, 1987–2003.
- Moore, J.G., 1987. Subsidence of the Hawaiian Ridge. *U. S. Geol. Surv. Prof. Pap.* 1350, 85–100.
- Morales, A.J., 1987. *Geología de las islas Robinson Crusoe y Santa Clara, Archipiélago Juan Fernández, V Región, Chile*. Bachelor Dissertation. Universidad Católica del Norte (103 pp.).
- Orozco, G., 2016. *Evolución estructural y tectónica de la isla Robinson Crusoe, Dorsal de Juan Fernández*. Master Dissertation. Universidad de Chile (94 pp.).
- Paquet, M., Day, J.M., Castillo, P.R., 2019. Osmium isotope evidence for a heterogeneous 3He/4He mantle plume beneath the Juan Fernandez Islands. *Geochim. Cosmochim. Acta* 261, 1–19.
- Pérez-Peña, J.V., Azañón, J.M., Azor, A., 2009. CalHypso: an ArcGIS extension to calculate hypsometric curves and their statistical moments. Applications to drainage basin analysis in SE Spain. *Comput. Geosci.* 35 (6), 1214–1223.
- Pimentel, A., Ramalho, R.S., Becerril, L., Larrea, P., Brown, R.J., 2020. Editorial: ocean island volcanoes: genesis, evolution and impact. *Front. Earth Sci.* 8, 82. <https://doi.org/10.3389/feart.2020.00082>.
- Plesner, S., Holm, P.M., Wilson, J.R., 2003. ⁴⁰Ar–³⁹Ar geochronology of Santo Antão, Cape Verde Islands. *J. Volcanol. Geotherm. Res.* 120 (2002), 103–121.
- Quartau, R., Trenhaile, A.S., Mitchell, N.C., Tempera, F., 2010. Development of volcanic insular shelves: insights from observations and modelling of Faial Island in the Azores Archipelago. *Mar. Geol.* 275, 66–83.
- Quartau, R., Hipolito, A., Romagnoli, C., Casalbore, D., Madeira, J., Tempera, F., Roque, C., Chiocci, F.L., 2014. The morphology of insular shelves as a key for understanding the geological evolution of volcanic islands: insights from Terceira Island (Azores). *Geochem. Geophys. Geosyst.* 15, 1801–1826.
- Quartau, R., Madeira, J., Mitchell, N.C., Tempera, F., Silva, P.F., Brandão, F., 2015. The insular shelves of the Faial Pico Ridge (Azores archipelago): a morphological record of its evolution. *Geochem. Geophys. Geosyst.* 16 (5), 1401–1420.
- Quartau, R., Trenhaile, A.S., Ramalho, R.S., Mitchell, N.C., 2018. The role of subsidence in shelf widening around ocean island volcanoes: insights from observed morphology and modeling. *Earth Planet. Sci. Lett.* 498, 408–417.
- Quensel, P., 1952. Additional comments on the geology of the Juan Fernandez Islands. In: Skottsberg, C. (Ed.), *The Natural History of Juan Fernandez and Easter Island*. Geography, Geology, Origin of Island Life vol. 1, pp. 37–88.
- Ramalho, R.S., 2011. *Building the Cape Verde Islands*. 1st edition. Springer (262 pp.).
- Ramalho, R.S., Quartau, R., Trenhaile, A.S., Mitchell, N.C., Woodroffe, C.D., Ávila, S.P., 2013. Coastal evolution on volcanic oceanic islands: a complex interplay between volcanism, erosion, sedimentation, sea-level change and biogenic production. *Earth-Sci. Rev.* 127, 140–170.
- Reyes, J., Lara, L.E., Morata, D., 2017. Contrasting P-T paths of shield and rejuvenated volcanism at Robinson Crusoe Island, Juan Fernández Ridge, SE Pacific. *J. Volcanol. Geotherm. Res.* 341, 242–254.
- Reyes, J., Lara, L.E., Hauff, F., Hoernle, K., Morata, D., Selles, D., Cooper, O., 2019. Petrogenesis of shield volcanism from the Juan Fernández Ridge, Southeast Pacific: melting of a low-temperature pyroxenite-bearing mantle plume. *Geochim. Cosmochim. Acta* 257, 311–335.
- Ricci, J., Lahitte, P., Quidelleur, X., 2015. Construction and destruction rates of volcanoes within tropical environment: examples from the Basse-Terre Island (Guadeloupe, Lesser Antilles). *Geomorphology* 228, 597–607.
- Robinson, J.E., Eakins, B.W., 2006. Calculated volumes of individual shield volcanoes at the young end of the Hawaiian Ridge. *J. Volcanol. Geotherm. Res.* 151 (1–3), 309–317.
- Rodrigo, C., Lara, L.E., 2014. Plate tectonics and the origin of the Juan Fernandez Ridge: analysis of bathymetry and magnetic patterns. *Lat. Am. J. Aquat. Res.* 42 (4), 907–917.
- Ryan, W.B.F., Carbotte, S.M., Coplan, J., O'Hara, S., Melkonian, A., Arko, R., Weissel, R.A., Ferrini, V., Goodwillie, A., Nitsche, F., Bonczkowski, J., Zemsky, R., 2009. Global Multi-Resolution Topography (GMRT) synthesis data set. *Geochem. Geophys. Geosyst.* 10, Q03014. <https://doi.org/10.1029/2008GC002332>.
- Salvany, T., Lahitte, P., Nativel, P., Gillot, P.Y., 2012. Geomorphological evolution of the Piton des Neiges volcano (Réunion Island, Indian Ocean): competition between volcanic construction and erosion since 1.4 Ma. *Geomorphology* 136 (1), 132–147.
- Samper, A., Quidelleur, X., Lahitte, P., Mollex, D., 2007. Timing of effusive volcanism and collapse events within an oceanic arc island: Basse-Terre, Guadeloupe archipelago (Lesser Antilles Arc). *Earth Planet. Sci. Lett.* 258 (1–2), 175–191.
- Sassolas-Serrayet, T., Cattin, R., Ferry, M., 2018. The shape of watersheds. *Nat. Commun.* 9, 3791. <https://doi.org/10.1038/s41467-018-06210-4>.
- Schmincke, H.U., 1982. Volcanic and chemical evolution of the Canary Islands. In: von Rad, U., et al. (Eds.), *Geology of the Northwestern African Continental Margin*. Springer-Verlag, Berlin, pp. 3–20.
- Schmincke, H.U., 2004. *Seamounts and Volcanic Islands in Volcanism*. 1st ed. Springer <https://doi.org/10.1007/978-3-642-18952-4>.
- Sepúlveda, P., Le Roux, J.P., Lara, L.E., Orozco, G., Astudillo, V., 2015. Biostatigraphic evidence for dramatic Holocene uplift of Robinson Crusoe Island, Juan Fernández Ridge, SE Pacific Ocean. *Biogeosciences* 12 (6), 1993–2001.
- Strahler, A., 1953. Hypsometry analysis of erosional topography. *Bull. Geol. Soc. Am.* 63, 923–938.

- Stuessy, T.F., Foland, K.A., Sutter, J.F., Sanders, R.W., Silva, M., 1984. Botanical and geological significance of potassium-argon dates from the Juan Fernandez Islands. *Science* 225 (80), 49–51. <https://doi.org/10.1126/science.225.4657.49>.
- Thomas, et al., 2012. Assessing subsidence rates and paleo water-depths for Tahiti reefs using U–Th chronology of altered corals. *Mar. Geol.* 295–298, 86–94.
- Thordarson, T., Garcia, M.O., 2018. Variance of the flexure model predictions with rejuvenated volcanism at Kilauea Point, Kaua'i, Hawai'i. *Front. Earth Sci.* 04. <https://doi.org/10.3389/feart.2018.00121>.
- Thouret, J.C., 1999. Volcanic geomorphology—an overview. *Earth Sci. Rev.* 47, 95–131.
- Trenhaile, A.S., 2000. Modeling the development of wave-cut shore platforms. *Mar. Geol.* 166 (1–4), 163–178.
- Truong, T.B., Castillo, P.R., Hilton, D.R., Day, J.M., 2018. The trace element and Sr–Nd–Pb isotope geochemistry of Juan Fernandez lavas reveal variable contributions from a high-³He/⁴He mantle plume. *Chem. Geol.* 476, 280–291.
- Vermeesch, P., 2009. Radialplotter: a java application for fission track, luminescence and other radial plots. *Radiat. Meas.* 44 (4), 409–410.
- Vogt, P.R., Smoot, N.C., 1984. The Geisha Guyots: multi-beam bathymetry and morphometric interpretation. *J. Geophys. Res.* 89, 11085–11107.
- Wadge, G., 1984. Comparison of volcanic production rates and subduction rates in the Lesser Antilles and Central America. *Geology* 12 (9), 555–558.
- White, S.M., Crisp, J.A., Spera, F.J., 2006. Long-term volumetric eruption rates and magma budgets. *Geochem. Geophys. Geosyst.* 7 (3).